

1 **Development of an orally available inhibitor of CLK1 for skipping a mutated dystrophin**
2 **exon in Duchenne muscular dystrophy**

3

4 Yukiya Sako¹, Kensuke Ninomiya¹, Yukiko Okuno², Masayasu Toyomoto¹, Atsushi Nishida³, Yuka
5 Koike^{1,†}, Kenji Ohe¹, Isao Kii^{1†}, Suguru Yoshida⁵, Naohiro Hashimoto⁴, Takamitsu Hosoya⁵,
6 Masafumi Matsuo³, Masatoshi Hagiwara^{1*}

7

8 ¹Department of Anatomy and Developmental Biology, Kyoto University Graduate School of
9 Medicine, Kyoto, Japan; ²Medical Research Support Centre, Kyoto University Graduate School
10 of Medicine, Kyoto, Japan; ³Department of Medical Rehabilitation, Faculty of Rehabilitation,
11 Kobegakuin University, Kobe, Japan; ⁴Department of Regenerative Medicine, National Centre for
12 Geriatrics and Gerontology, Oobu, Japan; ⁵Laboratory of Chemical Bioscience, Institute of
13 Biomaterials and Bioengineering, Tokyo Medical and Dental University, Tokyo, Japan.

14

15 †Current address: Pathophysiological and Health Science Team, Imaging Application Group,
16 Division of Bio-Function Dynamics Imaging, RIKEN Centre for Life Science Technologies, 6-7-3
17 Minatojima-minamimachi, Chuo-ku, Kobe, Hyogo 650-0047, Japan.

18

19 *Correspondence and requests for materials should be addressed to:

20 M.H. (hagiwara.masatoshi.8c@kyoto-u.ac.jp)

21 Duchenne muscular dystrophy (DMD) is a fatal progressive muscle-wasting disease.
22 Various attempts are underway to convert severe DMD to a milder phenotype by modulating the
23 splicing of the dystrophin gene and restoring its expression. In our previous study, we reported
24 TG003, an inhibitor of CDC2-like kinase 1 (CLK1), as a splice-modifying compound for
25 exon-skipping therapy; however, its metabolically unstable feature hinders clinical application.
26 Here, we show an orally available inhibitor of CLK1, named TG693, which promoted the skipping
27 of the endogenous mutated exon 31 in DMD patient-derived cells and increased the production
28 of the functional exon 31-skipped dystrophin protein. Oral administration of TG693 to mice
29 inhibited the phosphorylation of serine/arginine-rich proteins, which are the substrates of CLK1,
30 and modulated pre-mRNA splicing in the skeletal muscle. Thus, TG693 is a splicing modulator
31 for the mutated exon 31 of the dystrophin gene *in vivo*, possibly possessing therapeutic potential
32 for DMD patients.

33 **Introduction**

34 Duchenne muscular dystrophy (DMD) is an X-linked inherited neuromuscular disorder that
35 affects approximately 1 out of 3,500 newborn boys, and the most prevalent fatal muscle-wasting
36 disease¹⁻³. It is characterized by progressive muscle deterioration and wasting due to the
37 absence of dystrophin³. Unfortunately, DMD patients usually succumb to cardiac or respiratory
38 failure attributed to muscle dysfunction in their 20s, and no effective cure is currently available.
39 Nonsense mutations or deletions of exons, which cause frame shifts in the dystrophin mRNA and
40 generate premature termination codons (PTCs), usually result in the lack of dystrophin protein
41 and development of the disease.

42 Current therapeutic attempts to restore dystrophin protein expression include the induction
43 of exon skipping with antisense oligonucleotides (AONs)⁴⁻⁷ or small molecules (TG003)⁸ and the
44 suppression of nonsense-mediated mRNA decay, which includes the read-through of PTC (e.g.
45 Ataluren)^{9,10}, by chemical compounds. Several AONs have been designed as exon-skipping
46 therapies, in which ribosomes “skip” the mutated exons in pre-mRNA transcripts to produce an
47 in-frame, but truncated, transcript that is translated into a functional dystrophin protein¹¹⁻¹³.
48 However, considering their therapeutic cost and delivery efficiency to muscles, small chemical
49 compounds with exon-skipping function are highly anticipated for DMD therapy.

50 We previously reported on the small molecule TG003 that promotes skipping of dystrophin
51 exon 31 in cells harboring the c.4303G > T mutation⁸. In the patient’s muscle cells, two
52 dystrophin mRNA transcripts of different lengths are detected in nearly equal amounts—one with
53 the premature TAG termination codon in exon 31, and the other lacking only exon 31. The
54 dystrophin mRNA lacking the 111-bp exon 31 is in-frame to produce an internally deleted, but
55 functional dystrophin protein. The expression of the functional truncated protein is enhanced by
56 TG003 treatment.

57 Our initial findings showed that TG003 is an inhibitor of CDC-like-kinases (CLKs; CLK1, 2,
58 4)¹⁴, which phosphorylate stretches of alternating serine and arginine residues in
59 serine/arginine-rich (SR) protein family members^{15,16}. CLK-dependent phosphorylation of SR
60 proteins induces their association with transcribed RNAs¹⁷⁻¹⁹ to promote or, in some cases,

61 repress splice-site recognition, resulting in alternative splicing²⁰⁻²². Thus, TG003 acts by altering
62 mRNA splicing by inhibiting the phosphorylation of SR proteins^{14,23,24}.

63 Pharmacological efficacy in target tissues is an unavoidable issue for developing therapeutic
64 modalities. While TG003 was effective in modulating CLK activity and mRNA splicing in cellular
65 models of DMD⁸, its metabolic instability hinders its clinical application. In this study, we identified
66 an orally available selective CLK1 inhibitor, TG693, which promoted exon skipping and
67 production of a truncated functional dystrophin protein in immortalized cells derived from a
68 patient with DMD (c.4303G > T) to the same extent as TG003. Additionally, TG693 was
69 metabolically stable and transiently detected in the skeletal muscle at a bioactive level,
70 supporting its therapeutic potential as an orally available drug candidate.

71 **Results**

72 ***Development of the metabolically stable CLK1 inhibitor TG693***

73 We screened for stable exon-skipping inducers of the mutant DMD exon 31 (c.4303G > T) in our
74 original chemical library and identified the small molecule 5-(4-pyridinyl)-1H-indazole (henceforth
75 referred to as TG693) as an exon-skipping inducer (Fig. 1a). To test the in vivo stability of TG003
76 and TG693, mice were administered a single subcutaneous injection of either compound and
77 then serum concentrations were monitored by liquid chromatography-mass spectrometry
78 (LC/MS) at serial time points. While only trace amounts of TG003 were detected, the average
79 TG693 serum concentration was 13 μ M at 6 h post-injection, indicating that TG693 was more
80 stable than TG003 in the blood plasma (Fig. 1b). Subsequent analyses on CLK1 inhibition with in
81 vitro kinase assays revealed that TG693 inhibited the phosphorylation of a synthetic SRSF1 RS
82 domain peptide with a half-maximal inhibitory concentration (IC_{50}) of 112.6 nM, approximately
83 10-fold weaker than that of TG003 (IC_{50} = 13.1 nM) (Fig. 1c). We also examined whether TG693
84 served as an ATP-competitive inhibitor. Hanes-Woolf plots showed parallel lines with y-intercepts
85 that correspond to TG693 concentration, demonstrating that TG693 competes with ATP for a
86 single site in CLK1 (Fig. 1d; K_m = 14.88 μ M, K_i = 105.3 nM). Moreover, kinetic parameters
87 ($K_m^{apparent}$, $V_{max}^{apparent}$, α , α') were determined by Michaelis-Menten model fitting (Supplementary
88 Table S1), which indicated that TG693 was an ATP-competitive type I inhibitor that antagonized

89 CLK1. Further, in order to evaluate the specificity of TG693-mediated kinase, we investigated the
90 *in vitro* inhibitory activity of 1 μ M TG693 against a panel of 313 recombinant kinases. TG693
91 inhibited CLK1 and Haspin activity by over 90% and kinases over 50% inhibition were shown in a
92 kinase dendrogram (Fig. 1e). These suggested that TG693 was a potent and selective inhibitor
93 of CLK1.

94 ***TG693 inhibits CLK1 kinase activity in cells.***

95 TG003 administration to cultured cells inhibits the CLK1-mediated phosphorylation of SR
96 proteins, particularly that of SRSF4¹⁷. To examine the cellular activity of TG693, HeLa cells were
97 treated with increasing concentrations of compounds, and then SR protein phosphorylation was
98 assessed by western blotting with an anti-pan-phospho-SR antibody that recognizes canonical
99 SR protein family members²⁵. Notably, TG693 and TG003 inhibited the phosphorylation of
100 SRSF4 at 5 μ M and SRSF6 at 20 μ M and 10 μ M, respectively (Fig. 2a), confirming that these
101 compounds act via the same biochemical mechanism.

102 ***TG693 induces exon-skipping of a DMD splicing reporter.***

103 Since TG693 was shown to be a metabolically stable CLK1 inhibitor, we evaluated the
104 dose-dependent effects of TG693 on the skipping of mutant DMD exon 31 (c.4303G > T) with
105 HeLa cells expressing a H492-Dys Ex31m splicing reporter⁸. Interestingly, the effects of TG693
106 and TG003 on the exon-skipping were comparable, despite their differences in suppressing
107 CLK1 activity in *in vitro* kinase assays (Fig. 2b, upper panel); and TG693 had no effect on wild
108 type transcript splicing even at 30 μ M (Fig. 2c). To determine if this activity was specific to exon
109 31 mutation, we then evaluated the function of TG693 on exon-skipping with the
110 H492-dysEx27m splicing reporter containing a point deletion in exon 27 (c.3613delG
111 (p.Glu1205LysfsX9)) that causes in a frameshift-induced premature termination codon. As
112 shown in Supplementary Fig. S1, TG693 induced exon 27-skipping from H492-dysEx27m
113 reporter, similar to that previously observed with TG003⁸.

114 *CLK1* pre-mRNA splicing is regulated by CLK1 kinase activity¹⁴. In this mechanism,
115 abundant CLK1 levels induce SR phosphorylation, resulting in the removal of exon 4 from *CLK1*

116 pre-mRNA and nonsense-mediated mRNA decay^{26,27}. In previous reports, administration of
117 TG003 to cultured cells promoted full-length *CLK1* expression^{14,17}. Consistently, *CLK1* exon
118 4-skipped transcript expression was attenuated in the presence of 5 μ M TG693 (Fig. 2b, middle
119 panel), suggesting that TG693 exhibited a considerable inhibitory effect on CLK1 and
120 concomitant exon-skipping, similar to that of TG003⁸.

121 ***TG693 restored dystrophin expression in patient-derived cells***

122 We previously reported that TG003 restored dystrophin production in patient-derived myotubes⁸.
123 Therefore, we investigated the effect of TG693 on dystrophin expression in an immortalized cell
124 line derived from a DMD patient with the c.4303G > T mutation, which was by established by the
125 forced expression of constitutively active cyclin-dependent kinase 4, cyclin D1, and
126 telomerase^{28,29}. Notably, TG693 promoted the skipping of mutant exon 31 (Fig. 3a), but did not
127 affect any other exons (Supplementary Fig. S2 and Supplementary Table S4). Moreover, TG693
128 was sufficient to increase dystrophin protein expression in a dose-dependent manner with a 63%
129 and 38% increase at 10 and 20 μ M, respectively (Fig. 3b). Thus, these results supported the
130 therapeutic potential for TG693 in DMD patient cells harboring the c.4303G > T mutation in
131 dystrophin exon 31.

132 ***Oral administration of TG693 modulated splicing in mouse skeletal muscle***

133 To analyze the in vivo effects of TG693, mice were orally administered TG693 (30 mg kg⁻¹).
134 Notably, a significant amount of TG693 (>4 μ M) was detected in the tibialis anterior (TA) muscle
135 of mice (Fig. 4a), as well as a marked concomitant reduction of SR protein phosphorylation,
136 particularly that of SRSF4 (Fig. 4b). Further analysis of splicing modulation showed that TG693
137 promoted full-length *CLK1* transcript expression in TA, suggesting that treatment suppressed the
138 excision of exon 4 induced by CLK1 activity (Fig. 4c). TG693 was active in other muscle tissues,
139 such as the heart and diaphragm, as well as skeletal muscle (Fig. 4d). We also confirmed that
140 TG693 had no apparent toxicity in mice at up to 100 mg kg⁻¹ *per os* (Supplementary Fig. S3). No
141 mortalities or gross abnormalities were observed in TG693-treated animals during the
142 experimental period, nor did it affect body weight in mice administrated an overdose of the

143 compound. Thus, these results suggest that TG693 is a useful tool for inhibition of CLK1 activity
144 in vivo *per os*.

145 **Discussion**

146 We succeeded in identifying a selective ATP-competitive inhibitor of CLK1, named TG693.
147 TG693 is structurally distinct from TG003 (Fig. 1a), but it similarly shows potent CLK1 inhibition
148 as well as dystrophin exon 31 skipping enhancement in cells (Fig. 2a and Fig. 2b), strengthening
149 our original hypothesis that CLK1 can be the molecular target for splicing manipulation^{8,14}.
150 TG693 restored the dystrophin protein expression in cells harboring a point mutation (c.4303G >
151 T) in exon 31 of the dystrophin gene by inducing exon-skipping (Fig. 3). The c.4303G > T point
152 mutation in exon 31 attenuates exon recognition by disruption and creation of splicing elements
153 such as exonic splicing enhancer and silencer^{8,30,31}. Thus, mutated exon 31 is targeted by TG693
154 to suppress exon recognition without altering wild type transcript splicing (Fig. 2c). We also
155 showed TG693 promotes skipping of a mutated exon 27 in another patient (Supplementary Fig.
156 S1). In vivo mouse experiments revealed that oral TG693 administration decreased SR protein
157 phosphorylation in muscle tissue and modulated the splicing pattern of endogenous *Clk1* (Fig. 4).
158 Thus, these results indicated that TG693 could modulate the splicing pattern of the mutated
159 dystrophin gene in the patient by oral administration. This represents a significant advance in
160 drug-induced exon skipping therapy for DMD.

161 Splicing modulation has drawn increasing attention as a therapeutic strategy for DMD. In
162 2016, two antisense drugs that modulate splicing were approved by the U.S. Food and Drug
163 Administration (FDA) (e.g. Eteplirsen and Nusinersen), and exon-skipping therapy has become a
164 reality. While AONs offer a specific way to modulate splicing in a therapeutic manner, some
165 hurdles must be overcome for the orally available antisense drugs^{32,33}. Compared to AONs, small
166 chemical compounds may not be as specific, but more advantageous for the synthesis cost are
167 the oral availability. Thus, splicing modulation with small molecules can become an alternative
168 therapeutic approach in addition to AONs, and can expand applications of splicing modulation
169 therapy.

170 CLK1 inhibitors have attracted extensive attention in recent years. Notably, TG693 is the first
171 and only CLK1 inhibitor which is orally available and metabolically stable in blood^{34,35}. As such,
172 we believe that the present study will provide a foundation for the continued development of
173 therapies other diseases associated with aberrant CLK1 activity—such as Alzheimer’s and
174 Influenza^{36,37}.

175 Our results show that TG693 mediated CLK1 inhibition elicits changes in SR protein
176 phosphorylation, particularly that of SRSF4 and SRSF6 (Fig. 2a and Fig. 4b). SR proteins
177 regulate a multitude of splicing events in the phosphorylation dependent manner²¹, raising the
178 possibility that reduction of SR proteins phosphorylation may cause off-target splicing alteration.
179 Therefore, we previously checked transcriptional wide effect of TG003, which similarly inhibits
180 phosphorylation of SR proteins as TG693 *in vitro* (Fig. 2a), and we found that only 0.3% (110
181 /37487)²⁴ of registered alternative splicing events were skipped enhanced by TG003. TG693 is
182 fairly specific in its inhibition profile, showing significant off target effects (>70%) to only 4 of 313
183 kinases (Fig. 1e). This solidifies the mode-of-action evidence for TG693. Although we confirmed
184 TG693 had no apparent acute toxicity in mice at up to 100 mg kg⁻¹ *per os* (Supplementary Fig.
185 S3), more preclinical studies with other animal models are necessary to consider the clinical
186 application of TG693. We have also started a project to seek next generation CLK1 inhibitors
187 with a pharmaceutical company to improve the efficacy and selectivity of TG693 based on the
188 information written here.

189 TG693 is a simple compound with indazole and pyridine groups (Fig. 1a) far more
190 metabolically stable than TG003 which is a benzothiazole compound. We believe that TG003 is
191 easily metabolized via *O*-demethylation and subsequent sulfate conjugation of the hydroxyl
192 group³⁸ and likely interacts with CLK1 via hydrogen bonds in the ATP-binding pocket³⁹. In the
193 case of TG693, metabolically stable indazole moiety is suspected to form a hydrogen bond with
194 an amino acid residues of CLK1⁴⁰, but structural studies will be necessary to confirm this
195 hypothesis.

196 Our results suggest that exon-skipping therapy with orally available small molecule has
197 therapeutic potential to genetic diseases caused by disruption/creation of splicing elements,
198 including Duchenne muscular dystrophy. We believe that our approach is potentially applicable

199 to other genetic diseases caused by nonsense or frameshift mutations in the internal coding
200 exons whose length is a multiple of three. On this criteria, we found 6,244 pathogenic mutations
201 in the NIH ClinVar database that may be target candidates for exon-skipping therapy with TG693.
202 Our efforts have focused on expanding application of TG693 to other diseases, addition to the
203 Duchenne muscular dystrophy.

204 **Methods**

205 **Materials**

206 TG693 was synthesized as detailed in the Supporting Information. TG003 was prepared as
207 described previously¹⁴. Both compounds were dissolved in dimethylsulfoxide (DMSO)
208 (Hybri-MAX™, Sigma-Aldrich, St. Louis, MO, USA). Carboxymethyl cellulose sodium salt was
209 obtained from Nacalai Tesque (Kyoto, Japan).

210 **Antibodies**

211 The source and catalog numbers of commercially available primary antibodies have been
212 provided in Supplemental Table 2. Mouse monoclonal antibodies against phospho-SR proteins
213 (1H4) and α -tubulin (DM1A) were purchased from Invitrogen (Carlsbad, CA, USA) and Thermo
214 Fisher Scientific (Yokohama, Japan), respectively. Rabbit polyclonal antibody against dystrophin
215 was obtained from Abcam (Cambridge, UK). Goat polyclonal antibody against Lamin B (M-20)
216 was purchased from Santa Cruz Biotechnology (Santa Cruz, Dallas, TX, USA). HRP-conjugated
217 anti-rabbit, anti-goat IgG, and anti-mouse IgG secondary antibodies were purchased from GE
218 Healthcare Life Sciences (Pittsburgh, PA, USA), Jackson ImmunoResearch (West Grove, PA,
219 USA), and Abcam, respectively.

220 ***In vitro kinase assay***

221 CLK1 kinase activity was assessed as previously reported¹⁴ with minor modifications. The
222 reaction mixture containing serially diluted inhibitors, 10 mM MOPS-KOH (pH 6.5), 10 mM
223 magnesium chloride, 200 μ M EDTA, 1 μ M ATP, 0.167 μ Ci of [γ -³²P] ATP, 0.417 μ g of synthetic RS
224 peptide, and recombinant GST-tagged human CLK1 (Cat #04-126, Carna Biosciences, Kobe,
225 Japan) was prepared in a final volume of 25 μ L. The reaction mixture was incubated at 30 °C for
226 30 min, and phosphoric acid was added at a final concentration of 5% to stop the reaction. Then,
227 25 μ L of the reaction mixture was dispensed on a P81 phosphocellulose membrane (Cat
228 #20-134, Merck Millipore, Darmstadt, Germany) and washed four times in 5% phosphoric acid.
229 Cherenkov light from the incorporated ³²P was measured using a liquid scintillation counter. The
230 kinase assay conditions, including the incubation period and concentrations of kinases and

231 substrates, were optimized to maintain linearity during incubation. The net radioactivity was
232 determined by subtracting the background count from the reaction mixture without kinases. The
233 IC₅₀ of each compound was calculated by interpolation on a log-concentration-response curve
234 fitted with a four-parameter logistic equation.

235 ***Kinase profiling***

236 The effect of 1 μM TG693 on 263 kinases (listed in Supplementary Table S2) was examined with
237 immobilized metal ion affinity-based fluorescence polarization (IMAP) assay or off-chip mobility
238 shift assay (MSA) depending on the kinase being examined with an ATP concentration at the K_m
239 or 1 mM. These assays rely on the phosphorylation of small synthetic peptides developed for
240 each kinase, and detect activity by changes in electrophoretic mobility (MSA assay) or by binding
241 of a fluorescently labelled peptide to a large micro-particle and concomitant polarization
242 increases (IMAP assay). Reaction conditions for each kinase are described in Supplementary
243 Table S5. All kinase assays were carried out at Carna Biosciences (Kobe, Japan). The inhibitory
244 map was constructed using Kinome Render⁴¹.

245 ***Immobilized metal ion affinity-based fluorescence polarization (IMAP) Assay***

246 Substrate/ATP/metal (4×) and kinase (2×) solutions were prepared using with assay buffer (20
247 mM HEPES, 0.01% Tween-20, 2 mM DTT, pH 7.4), and then mixed in 384-well black plates for 1
248 hour at room temperature. IMAP binding solution (IMAP Screening Express kit; Molecular
249 Devices, Sunnyvale, CA, USA) was added to each well and incubated for 30 min. The level of
250 kinase activity was then evaluated by fluorescence polarization at 485/530 nm (Ex/Em).

251 ***Off-Chip Mobility Shift Assay (MSA)***

252 Inhibitor (4×), substrate/ATP-Metal (4×), and kinase (2×) solutions were prepared with assay
253 buffer (20 mM HEPES, 0.01% Triton X-100, 2 mM DTT, pH 7.5) and mixed in 384-well plates at
254 room temperature for 1 or 5 h depending on the kinase. Reactions were stopped by the addition
255 of termination buffer (QuickScout Screening Assist MSA; Carna Biosciences). The entire
256 reaction mixture was then applied to a LabChip system (Perkin-Elmer, Waltham, MA, USA) and

257 the product and substrate peptide peaks were separated and quantified, and then heights of
258 product (P) and substrate (S) peptide peaks were calculated. The level of kinase activity was
259 evaluated with the following equation: activity = P/(P+S).

260 ***ATP kinetics assay***

261 Kinetic reactions were performed with the same method used for in vitro kinase assays, except
262 that 0.05-0.4 μCi of [γ - ^{32}P] ATP was used. K_m and K_i values were calculated with a competitive
263 inhibition model in Prism 6 software (GraphPad Software, San Diego, CA, USA).

264 ***Plasmid construction, cell culture, and transfection***

265 The H492-dys Ex31m, H492-dys Ex31w, and H492-dys Ex27m plasmids were prepared as
266 described previously⁸. HeLa cells were maintained in low-glucose Dulbecco's modified Eagle's
267 medium (Nacalai Tesque) supplemented with 10% fetal bovine serum, 100 U/mL penicillin, and
268 100 $\mu\text{g}/\text{mL}$ streptomycin. Immortalized muscle cells from a DMD patient with the c.4303 G>T
269 mutation were established as described previously²⁸. Cells were maintained in Dulbecco's
270 modified Eagle's medium (Wako Pure Chemical Industries, Osaka, Japan) supplemented with
271 20% fetal bovine serum (Gibco, Grand Island, NY, USA), 2% Ultrosor™ G serum substitute (Pall
272 Corp., NY, USA), and 1% antibiotic-antimycotic solution (Gibco). Transfections were carried out
273 using Lipofectamine 2000 (Thermo Fisher Scientific) following the manufacturer's instructions.
274 For reporter assays, TG693 and TG003 were added to the culture medium for 24 h before
275 analysis.

276 ***RNA Isolation and Semiquantitative RT-PCR***

277 Total RNA was isolated from HeLa cells in 800 μL Sepasol-RNA I Super G (Nacalai Tesque)
278 and then treated with RQ1 RNase-free DNase (Promega, Madison, Wisconsin, USA) according
279 to the manufacturer's protocol. DMD patient-derived cells were lysed in 800 μL Trizol reagent
280 (Thermo Fisher Scientific) and then RNA was isolated with a Direct-zol RNA MiniPrep kit (Zymo
281 Research, Irvine, CA, USA). Tibialis anterior (TA) muscle homogenates were prepared using a
282 mortar and then RNA was isolated with an RNeasy MiniPrep kit (Qiagen, Hilgen,
283 Germany). First-strand cDNA was synthesized using Superscript II reverse transcriptase

284 (Invitrogen) and random hexamers (Takara Bio, Inc., Shiga, Japan). Semi-quantitative RT-PCR
285 was performed with Ex Taq polymerase (Takara Bio, Inc.) with the following cycle conditions:
286 95 °C for 2 min, followed by 32 (reporter and *Clk1*) or 25 cycles (*GAPDH*) of denaturation at
287 95 °C for 20 s, annealing at 58 °C for 20 s, and elongation at 72 °C for 1 min, with a final 5 min
288 incubation at 72 °C in a PCR thermal cycler (Bio-Rad Laboratories, Hercules, CA, USA). PCR
289 products were separated by electrophoresis and stained with ethidium bromide. Images were
290 obtained with a ChemiDoc™ MP Imaging System (Bio-Rad) and analyzed with Image Lab
291 software (Bio-Rad). Skipping efficiencies were determined by quantifying the skipped products
292 with a DNA 1000 LabChip Kit on an Agilent 2100 Bioanalyzer (Agilent Technologies, Santa Clara,
293 CA, USA). Exon skip/inclusion ratios were calculated as the amount of skipped transcript relative
294 to the sum the full-length and skipped transcript. The primers for semi-quantitative RT-PCR were
295 as follows: human *CLK1* forward, 5'-ATG AGA CAC TCA AAG AGA ACT TAC TG-3'; human
296 *CLK1* reverse, 5'-CTT TAT GAT CGA TGC ACT CCA C-3'; mouse *Clk1* forward, 5'-ATG AGA CAT
297 TCA AAG AGA ACT TAC TG-3'; mouse *Clk1* reverse, 5'-CAC TTT ATG ATC GAT GCA TTC C-3';
298 *GAPDH* forward, 5'-CCA TCA CCA TCT TCC AGG AGC GAG-3'; *GAPDH* reverse, 5'-GTG ATG
299 GCA TGG ACT GTG GTC ATG-3'; *dystrophin* forward, 5'-CCT GTA GCA CAA GAG GCC TTA-3';
300 *dystrophin* reverse, 5'-TCC ACA CTC TTT GTT TCC AAT G-3'; DMD splicing reporter forward,
301 5'-ATT ACT CGC TCA GAA GCT GTG TTG C-3'; and DMD splicing reporter reverse, 5'-AAG
302 TCT CTC ACT TAG CAA CTG GCA G-3'.

303 **Western blot analysis**

304 Proteins were extracted from HeLa cells, immortalized DMD cells, and mouse muscle tissue
305 using CellLytic M (Sigma-Aldrich, St. Louis, MO, USA), 1× Cell Lysis Buffer (Cell Signaling
306 Technology, Danvers, MA, USA), and CellLytic MT (Sigma-Aldrich), respectively. All buffers were
307 supplemented with protease and phosphatase inhibitor cocktail (#25955 and #0757461, Nacalai).
308 Protein concentrations were quantified with Protein Assay Reagent (Pierce by Thermo Fisher
309 Scientific). The HeLa cell and mouse tissue lysates were mixed with Sample buffer (#0949914,
310 Nacalai), denatured at 95 °C for 5 min, and then electrophoresed in a 10% SuperSep™ Ace gel
311 (Wako). The lysates of immortalized cells were mixed with NuPAGE LDS Sample buffer (Thermo

312 Scientific Fisher), denatured at 70 °C for 10 min, and electrophoresed in a 3-8% NuPAGE Novex
313 Tris-Acetate gels (Thermo Scientific Fisher). The samples were then transferred to PVDF
314 membranes (Pall Corporation, Port Washington, NY, USA). Antibody reactions were performed
315 with Can Get Signal[®] Immunoreaction Enhancer Solution (Toyobo, Osaka, Japan). Peroxidase
316 activities were visualized with ImmunoStar[®] LD (Wako) and a ChemiDoc[™] MP Imaging System
317 (Bio-Rad).

318 ***Mice and TG693/TG003 administration***

319 Seven-week-old, male Jcl:TCR mice were obtained from Charles River Laboratories (Shiga,
320 Japan). All procedures were performed in accordance with the US National Institutes of Health
321 Guide for the Care and Use of Laboratory Animals and approved by the Institutional Animal Care
322 and Use Committee of Kyoto University Graduate School of Medicine. Mice were
323 subcutaneously injected with 30 mg kg⁻¹ TG693 or TG003 suspended in 5% DMSO, 5% Solutol,
324 9% Tween-80, and 81% saline. TG693 was also administered orally at a dose of 30 mg kg⁻¹
325 suspended in 0.5% carboxymethylcellulose.

326 ***In vivo pharmacokinetic analysis***

327 TG693 metabolism and tissue bioavailability were assessed in mouse plasma and muscle tissue.
328 To collect plasma, mice were anesthetized with isoflurane (Mylan, Osaka, Japan) at the indicated
329 time point. Whole blood samples were collected, allowed to clot, and then centrifuged to isolate
330 serum. TG693 or TG003 serum levels were analyzed by LC/MS with an Agilent 6420 Q-TOF
331 mass spectrometer (Agilent Technologies) and ZORBAX HILIC Plus (TG693) or ZORBAX
332 Eclipse Plus C18 (TG003) columns (Agilent Technologies). For muscle tissue bioavailability,
333 mice were sacrificed by cervical dislocation and the tibialis anterior (TA) muscles, heart, and
334 diaphragm dissected. TA homogenates were prepared using a Bead Crusher μ T-12 shaking
335 machine (Taitec, Kyoto, Japan) in saline and used to assess TG693 levels by LC/MS with a
336 Poroshell 120 PFP (Agilent Technologies).

337 ***Statistical analysis***

338 Statistical analysis was performed using Student's t-tests, except for the comparison of
339 exon-skipping ratio in patient-derived cells analyzed by one-way ANOVA with independent *post*
340 *hoc* Tukey's multiple comparison testing. Results are reported as the means \pm SD. Statistical
341 significance was defined as $p < 0.05$. IC₅₀ values were calculated from data fitted to a
342 four-parameter logistic curve (variable slope) in Prism 6.0 software.

343 **References**

- 344 1 Duchenne, G. B. The Pathology of Paralysis with Muscular Degeneration (Paralysie
345 Myosclerotique), or Paralysis with Apparent Hypertrophy. *Br Med J* **2**, 541-542 (1867).
- 346 2 Zellweger, H. & Antonik, A. Newborn screening for Duchenne muscular dystrophy. *Pediatrics*
347 **55**, 30-34 (1975).
- 348 3 Hoffman, E. P., Brown, R. H., Jr. & Kunkel, L. M. Dystrophin: the protein product of the
349 Duchenne muscular dystrophy locus. *Cell* **51**, 919-928 (1987).
- 350 4 Matsuo, M. Duchenne/Becker muscular dystrophy: from molecular diagnosis to gene therapy.
351 *Brain Dev* **18**, 167-172 (1996).
- 352 5 Wood, M. J., Gait, M. J. & Yin, H. RNA-targeted splice-correction therapy for neuromuscular
353 disease. *Brain* **133**, 957-972 (2010).
- 354 6 Aartsma-Rus, A. & van Ommen, G. J. Less is more: therapeutic exon skipping for Duchenne
355 muscular dystrophy. *Lancet Neurol* **8**, 873-875 (2009).
- 356 7 Le Roy, F., Charton, K., Lorson, C. L. & Richard, I. RNA-targeting approaches for
357 neuromuscular diseases. *Trends Mol Med* **15**, 580-591 (2009).
- 358 8 Nishida, A. *et al.* Chemical treatment enhances skipping of a mutated exon in the dystrophin
359 gene. *Nat Commun* **2**, 308 (2011).
- 360 9 Welch, E. M. *et al.* PTC124 targets genetic disorders caused by nonsense mutations. *Nature*
361 **447**, 87-91 (2007).
- 362 10 Malik, V. *et al.* Gentamicin-induced readthrough of stop codons in Duchenne muscular
363 dystrophy. *Ann Neurol* **67**, 771-780 (2010).
- 364 11 Takeshima, Y. *et al.* Intravenous infusion of an antisense oligonucleotide results in exon
365 skipping in muscle dystrophin mRNA of Duchenne muscular dystrophy. *Pediatr Res* **59**,
366 690-694 (2006).
- 367 12 Takeshima, Y., Nishio, H., Sakamoto, H., Nakamura, H. & Matsuo, M. Modulation of in vitro
368 splicing of the upstream intron by modifying an intra-exon sequence which is deleted from the
369 dystrophin gene in dystrophin Kobe. *J Clin Invest* **95**, 515-520 (1995).
- 370 13 Pramono, Z. A. *et al.* Induction of exon skipping of the dystrophin transcript in
371 lymphoblastoid cells by transfecting an antisense oligodeoxynucleotide complementary to an
372 exon recognition sequence. *Biochem Biophys Res Commun* **226**, 445-449 (1996).
- 373 14 Muraki, M. *et al.* Manipulation of alternative splicing by a newly developed inhibitor of Clks.
374 *J Biol Chem* **279**, 24246-24254 (2004).
- 375 15 Colwill, K. *et al.* The Clk/Sty protein kinase phosphorylates SR splicing factors and regulates
376 their intranuclear distribution. *EMBO J* **15**, 265-275 (1996).
- 377 16 Johnson, K. W. & Smith, K. A. Molecular cloning of a novel human cdc2/CDC28-like protein

378 kinase. *J Biol Chem* **266**, 3402-3407 (1991).

379 17 Ninomiya, K., Kataoka, N. & Hagiwara, M. Stress-responsive maturation of Clk1/4
380 pre-mRNAs promotes phosphorylation of SR splicing factor. *The Journal of cell biology* **195**,
381 27-40 (2011).

382 18 Prasad, J. & Manley, J. L. Regulation and substrate specificity of the SR protein kinase
383 Clk/Sty. *Mol Cell Biol* **23**, 4139-4149 (2003).

384 19 Aubol, B. E. *et al.* N-terminus of the protein kinase CLK1 induces SR protein
385 hyperphosphorylation. *Biochem J* **462**, 143-152 (2014).

386 20 Shepard, P. J. & Hertel, K. J. The SR protein family. *Genome Biol* **10**, 242 (2009).

387 21 Long, J. C. & Caceres, J. F. The SR protein family of splicing factors: master regulators of
388 gene expression. *Biochem J* **417**, 15-27 (2009).

389 22 Pandit, S. *et al.* Genome-wide analysis reveals SR protein cooperation and competition in
390 regulated splicing. *Mol Cell* **50**, 223-235 (2013).

391 23 Yomoda, J. *et al.* Combination of Clk family kinase and SRp75 modulates alternative splicing
392 of Adenovirus E1A. *Genes Cells* **13**, 233-244 (2008).

393 24 Sakuma, M., Iida, K. & Hagiwara, M. Deciphering targeting rules of splicing modulator
394 compounds: case of TG003. *BMC Mol Biol* **16**, 16 (2015).

395 25 Neugebauer, K. M., Stolk, J. A. & Roth, M. B. A conserved epitope on a subset of SR proteins
396 defines a larger family of Pre-mRNA splicing factors. *The Journal of cell biology* **129**, 899-908
397 (1995).

398 26 Duncan, P. I., Stojdl, D. F., Marius, R. M., Scheit, K. H. & Bell, J. C. The Clk2 and Clk3
399 dual-specificity protein kinases regulate the intranuclear distribution of SR proteins and
400 influence pre-mRNA splicing. *Exp Cell Res* **241**, 300-308 (1998).

401 27 Duncan, P. I., Stojdl, D. F., Marius, R. M. & Bell, J. C. In vivo regulation of alternative
402 pre-mRNA splicing by the Clk1 protein kinase. *Mol Cell Biol* **17**, 5996-6001 (1997).

403 28 Nishida, A. *et al.* Staurosporine allows dystrophin expression by skipping of
404 nonsense-encoding exon. *Brain Dev* **38**, 738-745 (2016).

405 29 Shiomi, K. *et al.* CDK4 and cyclin D1 allow human myogenic cells to recapture growth
406 property without compromising differentiation potential. *Gene Ther* **18**, 857-866 (2011).

407 30 Zhu, J., Mayeda, A. & Krainer, A. R. Exon identity established through differential
408 antagonism between exonic splicing silencer-bound hnRNP A1 and enhancer-bound SR
409 proteins. *Mol Cell* **8**, 1351-1361 (2001).

410 31 Okunola, H. L. & Krainer, A. R. Cooperative-binding and splicing-repressive properties of
411 hnRNP A1. *Mol Cell Biol* **29**, 5620-5631 (2009).

412 32 Havens, M. A. & Hastings, M. L. Splice-switching antisense oligonucleotides as therapeutic
413 drugs. *Nucleic Acids Res* **44**, 6549-6563 (2016).

414 33 Murakami, M. & Watanabe, C. Can colorectal delivery technology provide a platform for
415 enteral oligonucleotide-based therapeutics? *Drug Discov Ther* **10**, 273-275 (2016).

416 34 Naert, G. *et al.* Leucettine L41, a DYRK1A-preferential DYRKs/CLKs inhibitor, prevents
417 memory impairments and neurotoxicity induced by oligomeric Abeta25-35 peptide
418 administration in mice. *Eur Neuropsychopharmacol* **25**, 2170-2182 (2015).

419 35 Bidinosti, M. *et al.* CLK2 inhibition ameliorates autistic features associated with SHANK3
420 deficiency. *Science* **351**, 1199-1203 (2016).

421 36 Jain, P. *et al.* Human CDC2-like kinase 1 (CLK1): a novel target for Alzheimer's disease. *Curr*
422 *Drug Targets* **15**, 539-550 (2014).

423 37 Karlas, A. *et al.* Genome-wide RNAi screen identifies human host factors crucial for influenza
424 virus replication. *Nature* **463**, 818-822 (2010).

425 38 Masaki, S. *et al.* Design and synthesis of a potent inhibitor of class 1 DYRK kinases as a
426 suppressor of adipogenesis. *Bioorg Med Chem* **23**, 4434-4441 (2015).

427 39 Ogawa, Y. *et al.* Development of a novel selective inhibitor of the Down syndrome-related
428 kinase Dyrk1A. *Nat Commun* **1**, 86 (2010).

429 40 Bamborough, P. *et al.* N-4-Pyrimidinyl-1H-indazol-4-amine inhibitors of Lck: indazoles as
430 phenol isosteres with improved pharmacokinetics. *Bioorg Med Chem Lett* **17**, 4363-4368
431 (2007).

432 41 Chartier, M., Chenard, T., Barker, J. & Najmanovich, R. Kinome Render: a stand-alone and
433 web-accessible tool to annotate the human protein kinome tree. *PeerJ* **1**, e126 (2013).

434

435 **Acknowledgements**

436 We thank the members of the M.H. laboratory for experimental assistance, helpful discussions,
437 and comments. We also acknowledge Dr. Shin'ichi Takeda and the members of his lab,
438 especially Dr. Yoshitsugu Aoki and Dr. Takashi Saito, at the National Centre of Neurology and
439 Psychiatry (NCNP) for technical advice. We are grateful to Dr. Kei Iida, Dr. Akihide Takeuchi,
440 Motoyasu Hosokawa, Maki Sakuma, Kohei Araki, and Keiko Hayashi at Kyoto University for their
441 helpful comments and experimental assistance. We also thank the Radioisotope Research
442 Centre and Medical Research Support Centre at Kyoto University for instrumental support.
443 Illustrations were reproduced courtesy of Cell Signaling Technology, Inc. This study was
444 supported by Grants-in-Aid for Scientific Research from the Japan Society for the Promotion of
445 Science (Grant No. 15H05721 to M.H. and 15K10050 to K.O.), the Research Program of
446 Innovative Cell Biology (No. 231006 to M.H.), the National Institute of Biomedical Innovation
447 (NIBIO, No. 241011 to M.H.), and Intramural Research Grant 25-5 for Neurological and
448 Psychiatric Disorder of NCNP (to M.H.).

449 **Author Contributions**

450 Y.S., K.N., K.O., I.K., and T.H. designed the study. Y.S. performed experiments and analyzed the
451 data. K.N. performed the compound screening. Y.O. assisted with the ATP kinetics assay. M.T.
452 assisted with the pharmacokinetic assay in mouse skeletal muscle. Y.K. performed the
453 pharmacokinetic assay with mouse whole blood. S.Y. and T.H. synthesized small molecules. N.H.
454 and M.M. generated the immortalized patient-derived cells. A.N. and M.M. constructed of the
455 reporter vector and performed RT-PCR and western blotting. Y.S., K.N., K.O., and I.K. wrote the
456 manuscript. S.Y., T.H., and M.H. provided feedback during manuscript preparation. M.H.
457 supervised the study.

458 **Competing Financial Interests**

459 The authors declare no competing financial interests.

460 **Figure legends**

461 **Figure 1. TG693 is a metabolically stable CDC2-like kinase 1 (CLK1) inhibitor.**

462 (a) TG693 and TG003 chemical structures. (b) Pharmacokinetic profile of TG693 after a single
463 30 mg kg⁻¹ dose administered by subcutaneous injection in imprinting control region (ICR) mice.
464 Data indicate the mean ± SEM (n = 3). (c) Recombinant CLK1 was incubated with the substrate
465 peptide in the presence of the indicated concentrations of small molecules. Data represent the
466 means ± SD (n = 3). Representative dose-response curves with Hill slopes are shown. (d)
467 TG693 competitive ATP inhibition is shown in Michaelis-Menten (left) and Hanes-Woolf (right)
468 plots. CLK1 kinase activity was measured at the indicated concentrations of TG693 and ATP.
469 Velocity was plotted versus [ATP] and [ATP]/velocity was plotted versus [ATP]. (e) Map of the
470 inhibitory activities of TG693 on a kinase dendrogram. Percent inhibition by 1 μM TG693 was
471 measured for a panel of 313 kinases. Red circles indicate the inhibited kinases and are sized
472 according to percent inhibition. The illustration was reproduced courtesy of Cell Signaling
473 Technology, Inc. (www.cellsignal.com).

474 **Figure 2. TG693 promotes skipping of mutated exon 31 in HeLa cells in a dose-dependent**
475 **manner.**

476 (a) SR protein phosphorylation was assessed in HeLa cells treated with TG693 and TG003 for 1
477 h. Lamin B served as a loading control. Uncropped images have been provided in
478 Supplementary Fig. S4. (b, c) Effect of TG693 on exon 31 skipping with the reporter plasmid.
479 Transfected HeLa cells were incubated in the presence of TG693, TG003, or DMSO vehicle for
480 24 h. Reporter and endogenous *Clk1* splicing was then analyzed by RT-PCR. *GAPDH* served as
481 a control. The Splicing ratios were quantified by intensity analysis and normalized to *GAPDH*
482 expression. Uncropped images have been provided in Supplementary Fig. S5 and
483 Supplementary Fig. S6, respectively. Data represent the means ± SD (n = 3).

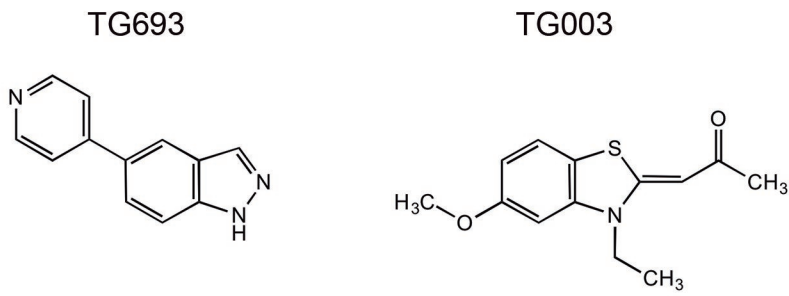
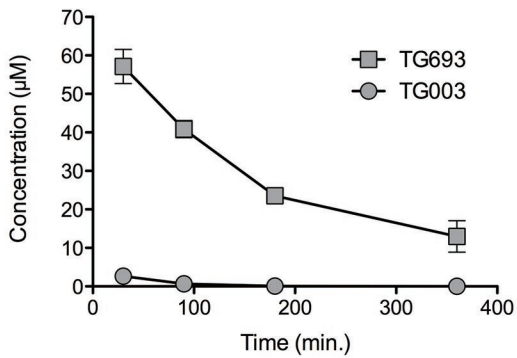
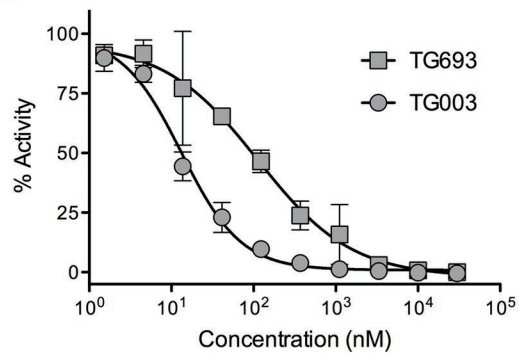
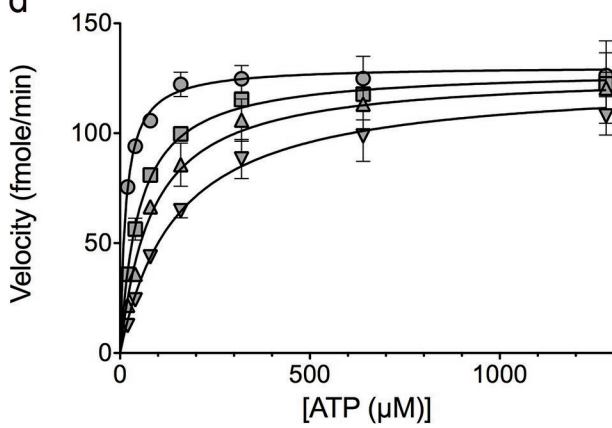
484 **Figure 3. TG693 induces truncated dystrophin protein expression in patient-derived cells.**

485 Immortalized DMD patient-derived cells were treated with increasing concentrations of TG693 for

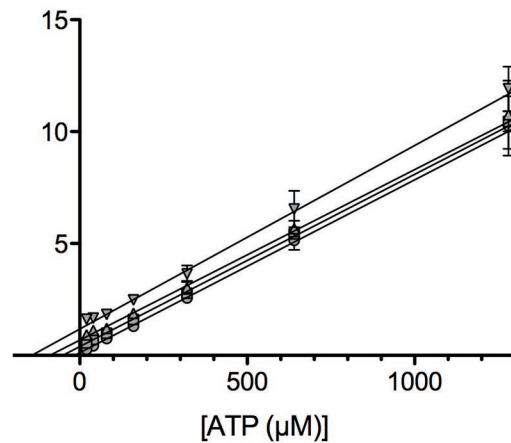
486 2 d. (a) Semi-quantitative RT-PCR for dystrophin exon skipping. The uncropped image is
487 provided in Supplementary Fig. S7. Data represent the means \pm SD (n = 3). * p < 0.05. (b)
488 Western blotting of dystrophin protein expression in TG693-treated cells using
489 C-terminal-directed antibody. α -Tubulin was used as a loading control. Uncropped images have
490 been provided in Supplementary Fig. S8. Data are representative of three independent
491 experiments.

492 **Figure 4. TG693 effect as a CLK1 inhibitor in the mouse tibialis anterior muscle.**

493 (a) TG693 bioavailability in the tibialis anterior (TA) muscle of ICR mice after oral administration
494 of a single 30 mg kg⁻¹ dose. Data represent the mean \pm SEM (n = 3). (b) SR protein
495 phosphorylation status in the TA muscle of ICR mice after oral administration. Lamin B served as
496 a loading control. SRSF4 phosphorylation was quantified by densitometry. Uncropped images
497 are provided in Supplementary Fig. S9. Data represent means \pm SD (n = 5). * p < 0.05. (c, d) *Clk1*
498 *expression* in the TA muscle, heart and diaphragm were analyzed by RT-PCR with a *GAPDH*
499 internal control. Uncropped images are provided in Supplementary Fig. S10 and in
500 Supplementary Fig. S11, respectively. Data represent the means \pm SD (n = 3). * p < 0.05.

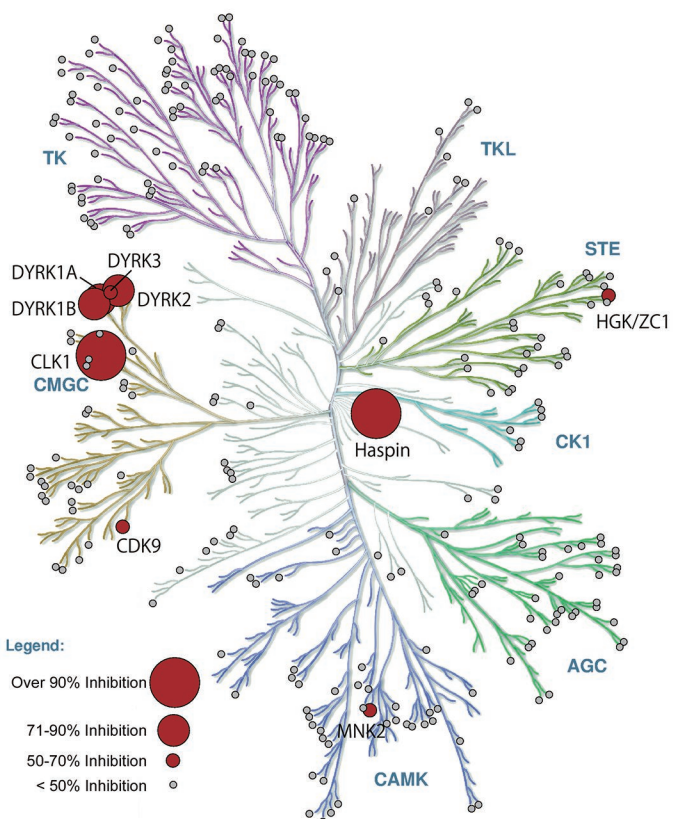
a**b****c****d**

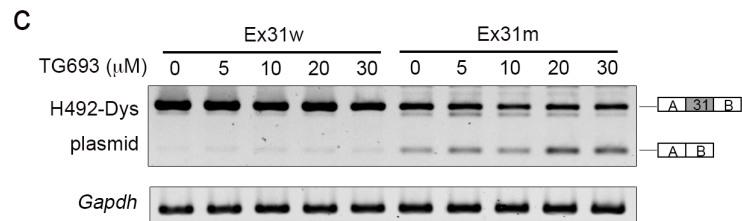
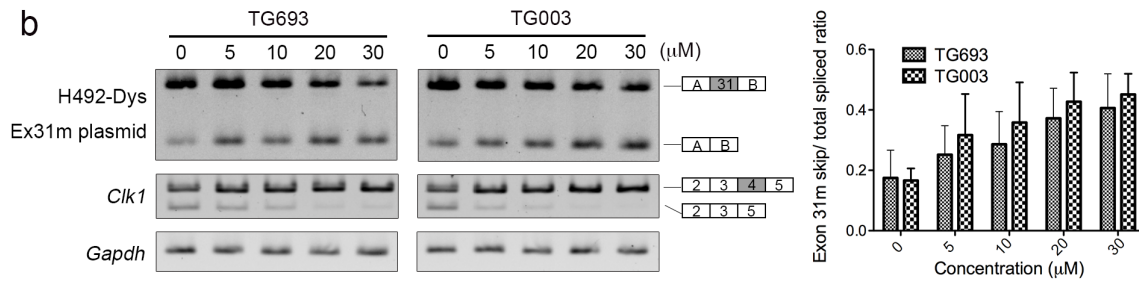
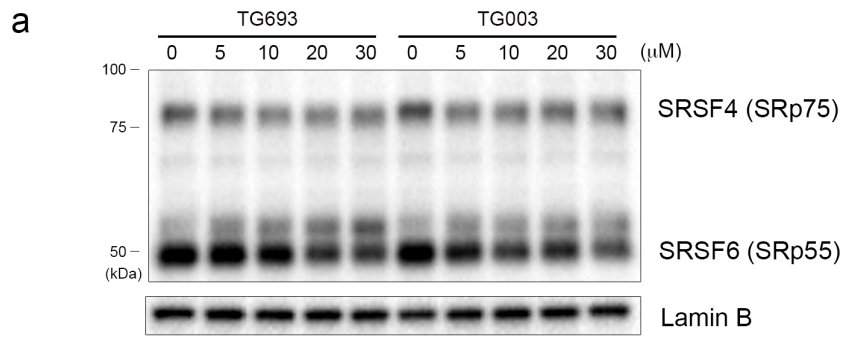
[ATP (µM)] / Velocity (fmole/min)



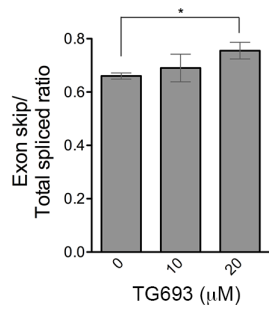
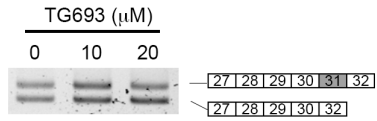
Concentration of TG693

- 0 nM
- 250 nM
- ▲ 500 nM
- ▼ 1000 nM

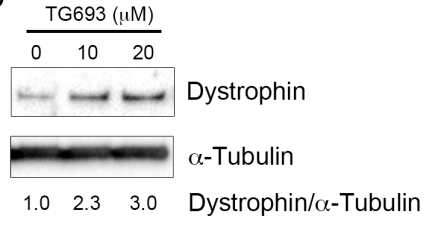
e

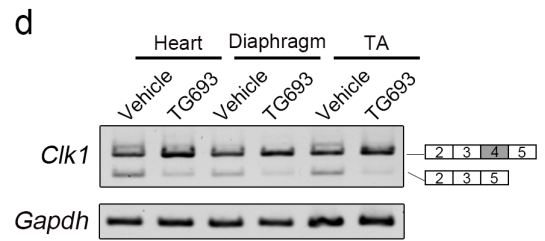
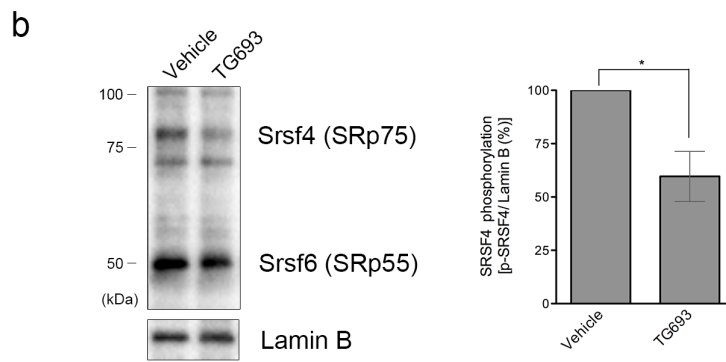
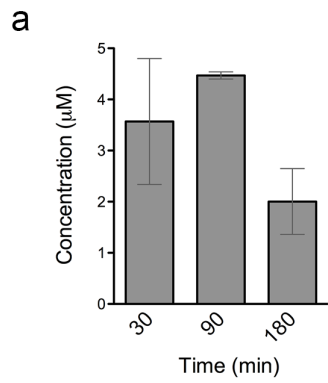


a



b





Supporting Information

Development of an orally available inhibitor of CLK1 for skipping a mutated dystrophin exon in Duchenne muscular dystrophy

Yukiya Sako¹, Kensuke Ninomiya¹, Yukiko Okuno², Masayasu Toyomoto¹, Atsushi Nishida³, Yuka Koike^{1,†}, Kenji Ohe¹, Isao Kii^{1†}, Suguru Yoshida⁵, Naohiro Hashimoto⁴, Takamitsu Hosoya⁵, Masafumi Matsuo³, Masatoshi Hagiwara^{1*}

*Correspondence: hagiwara.masatoshi.8c@kyoto-u.ac.jp

¹Department of Anatomy and Developmental Biology, Kyoto University Graduate School of Medicine, Kyoto, Japan; ²Medical Research Support Centre, Kyoto University Graduate School of Medicine, Sakyo-ku, Kyoto 606-8501, Japan; ³Department of Medical Rehabilitation, Faculty of Rehabilitation, Kobegakuin University, Kobe, Hyogo, Japan;

⁴Department of Regenerative Medicine, National Centre for Geriatrics and Gerontology, 7-430 Morioka, Oobu, Aichi 474-8522, Japan; ⁵Laboratory of Chemical Bioscience, Institute of Biomaterials and Bioengineering, Tokyo Medical and Dental University, Tokyo, Japan.

[†]Current address: Pathophysiological and Health Science Team, Imaging Application Group, Division of Bio-Function Dynamics Imaging, RIKEN Centre for Life Science Technologies, 6-7-3 Minatojima-minamimachi, Chuo-ku, Kobe, Hyogo 650-0047, Japan.

***Contact information**

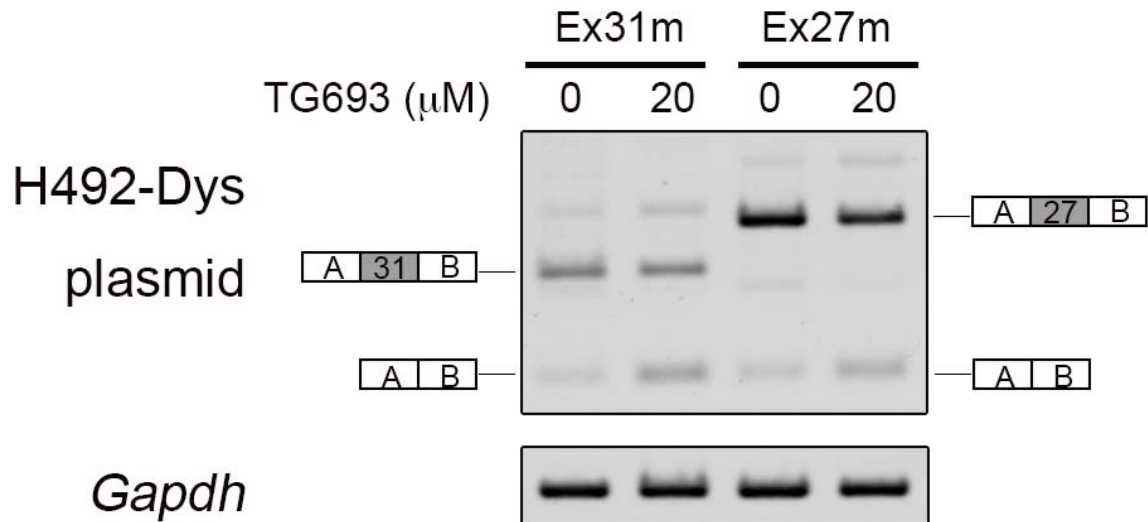
Masatoshi Hagiwara, MD and PhD

Department of Anatomy and Developmental Biology, Graduate School of Medicine, Kyoto University, Yoshida-Konoe-cho, Sakyo-ku, Kyoto 606-8501, Japan

E-mail: hagiwara.masatoshi.8c@kyoto-u.ac.jp

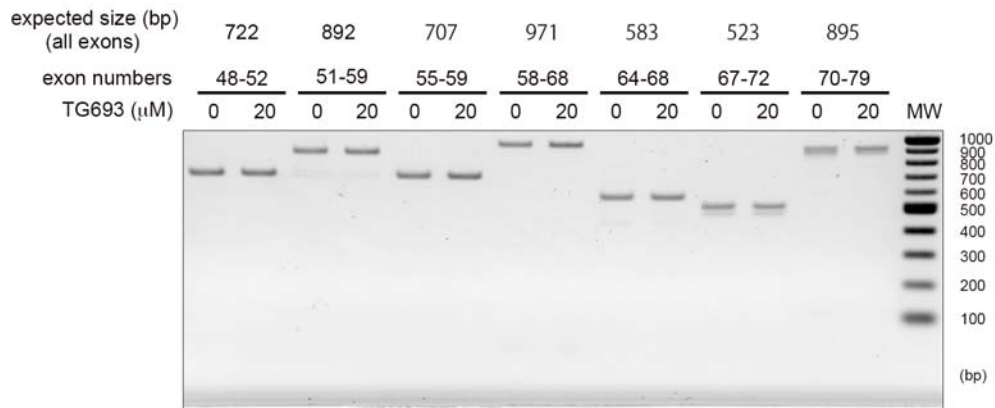
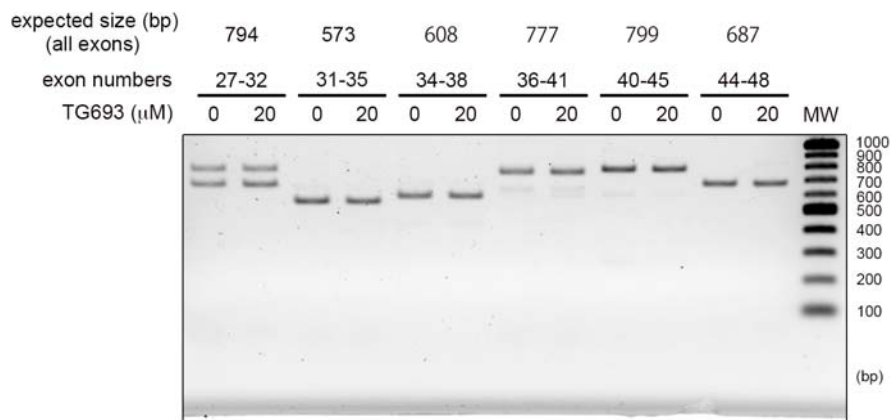
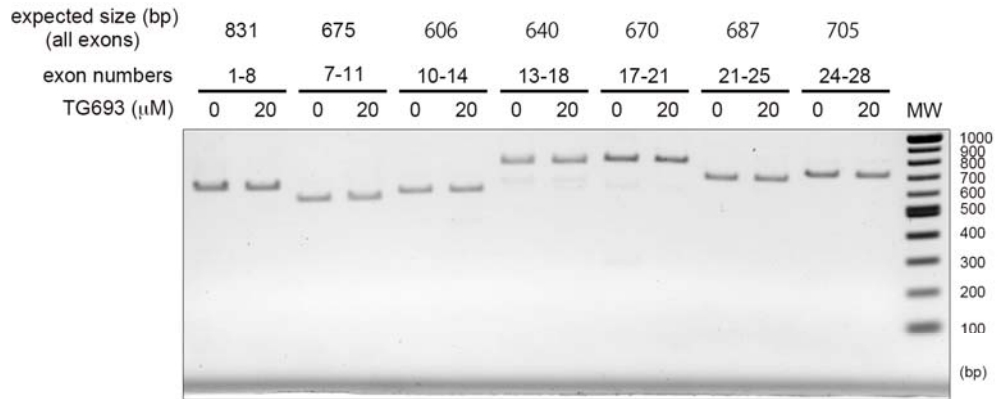
Tel: +81-75-753-4341 and Fax: +81-75-751-7529

Supporting Figures



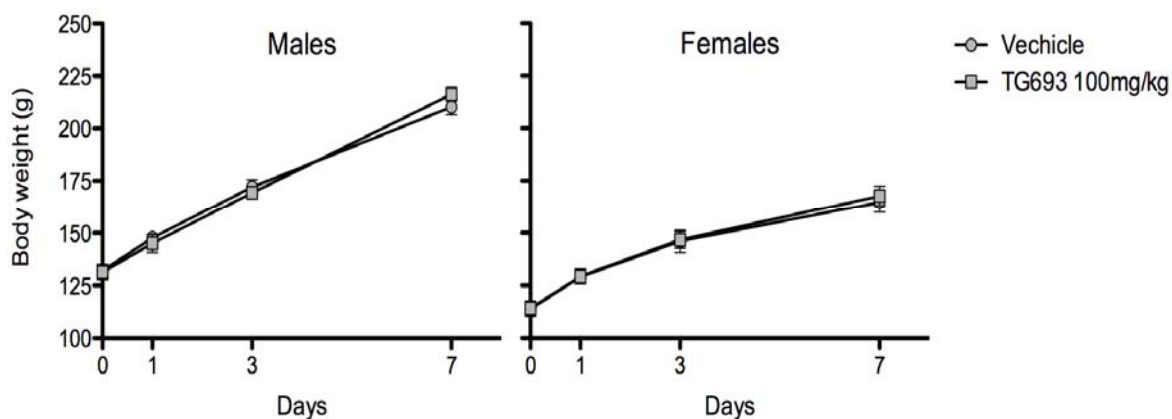
Supplementary figure S1. TG693 also promotes the skipping of a mutated exon27 in HeLa cells.

Effect of TG693 on exon 27 skipping was examined using the reporter plasmid. Transfected HeLa cells were incubated in the presence of TG693 or DMSO vehicle for 24 h. Reporter was then analyzed by RT-PCR. *GAPDH* served as a control. Uncropped images have been provided in Supplementary Fig.S12. Data are representative of three independent experiments.



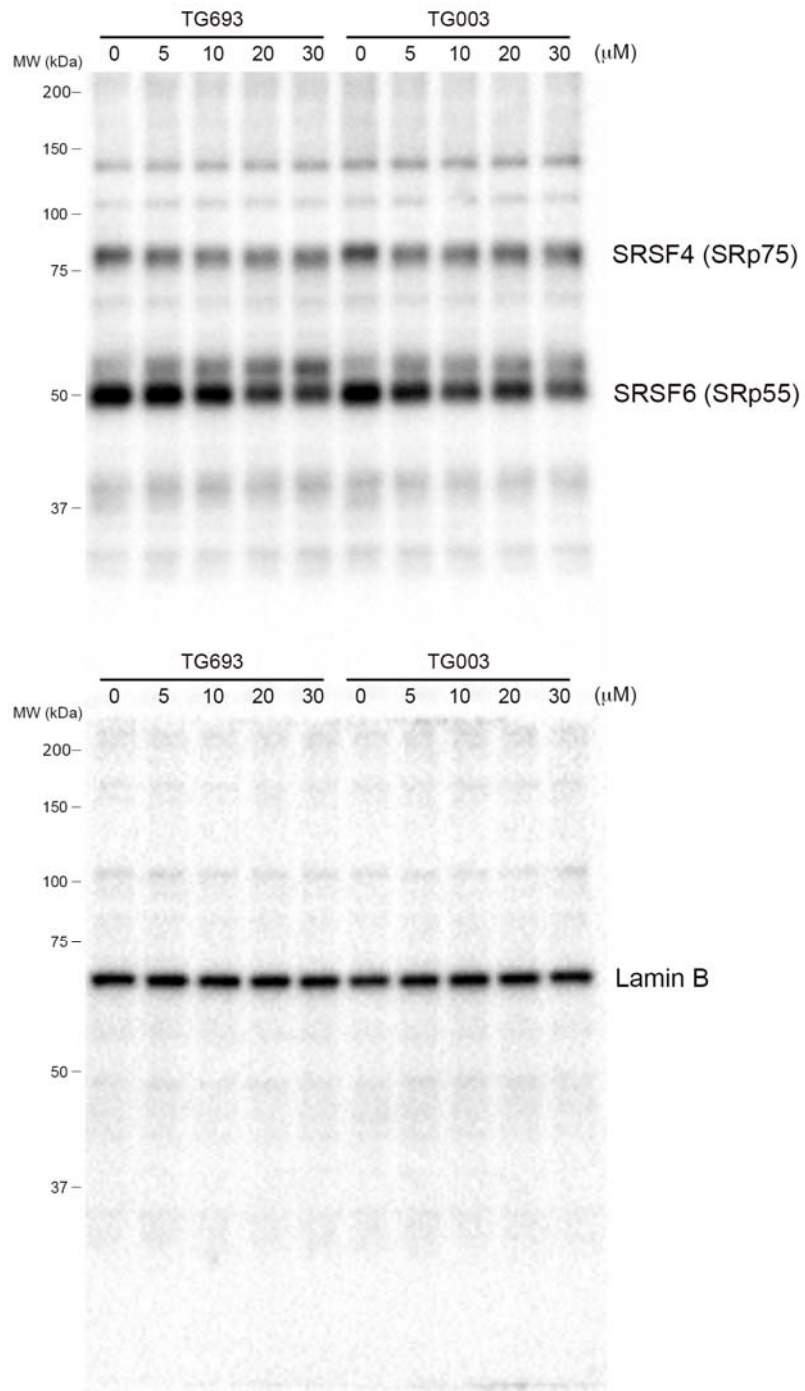
Supplementary figure S2. TG693 specifically induces skipping of the mutated exon 31 and has almost no effect on splicing of other dystrophin introns in patient-derived cells.

Immortalized DMD patient-derived cells were treated with 20 μ M of TG693 for 2 d. RT-PCR for dystrophin exons. The numbers of exons amplified by specific primer combinations are indicated above the lanes. Uncropped images have been provided in Supplementary Fig.S13.

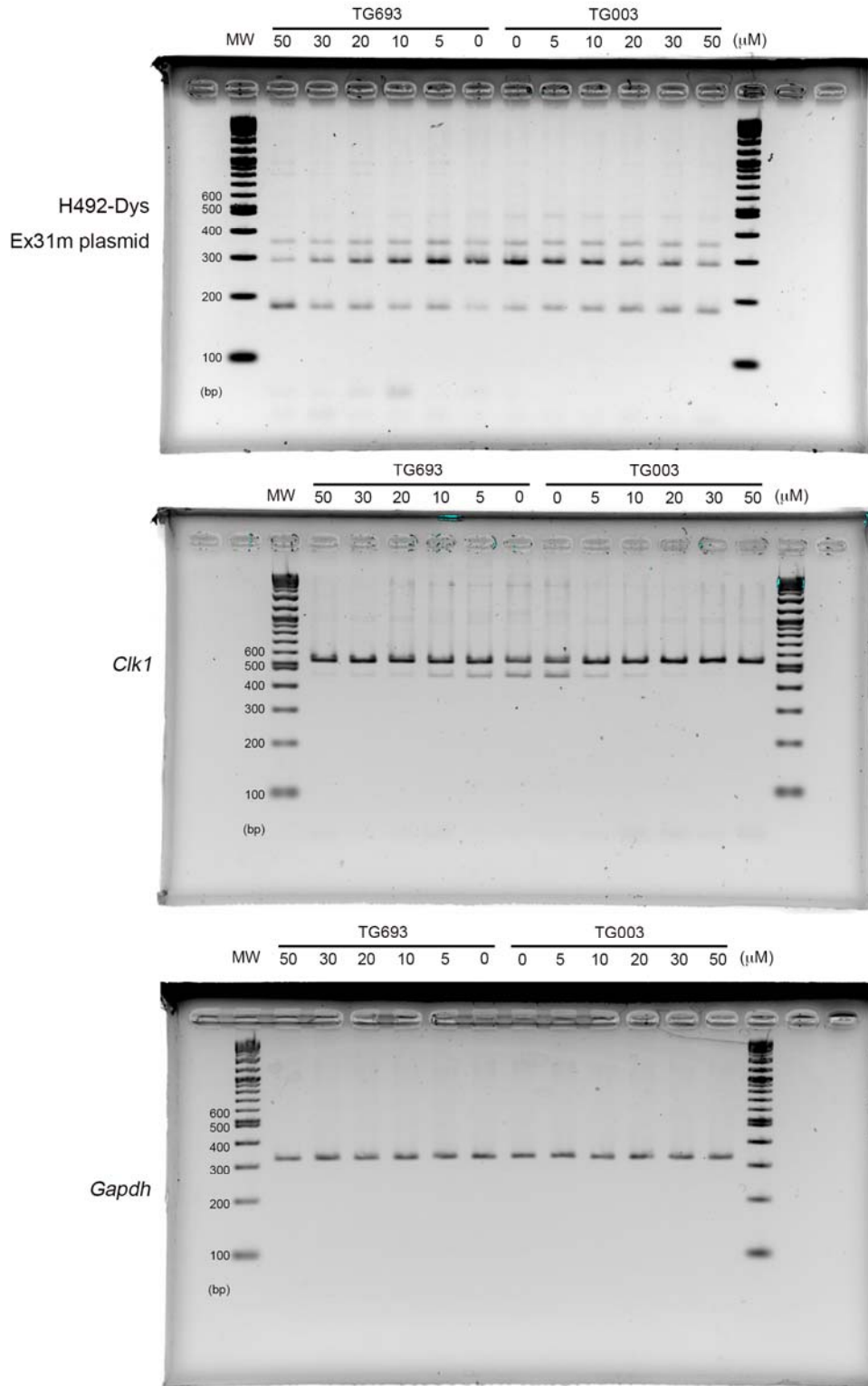


Supplementary figure S3. For seven days single dose oral toxicity studies in rats

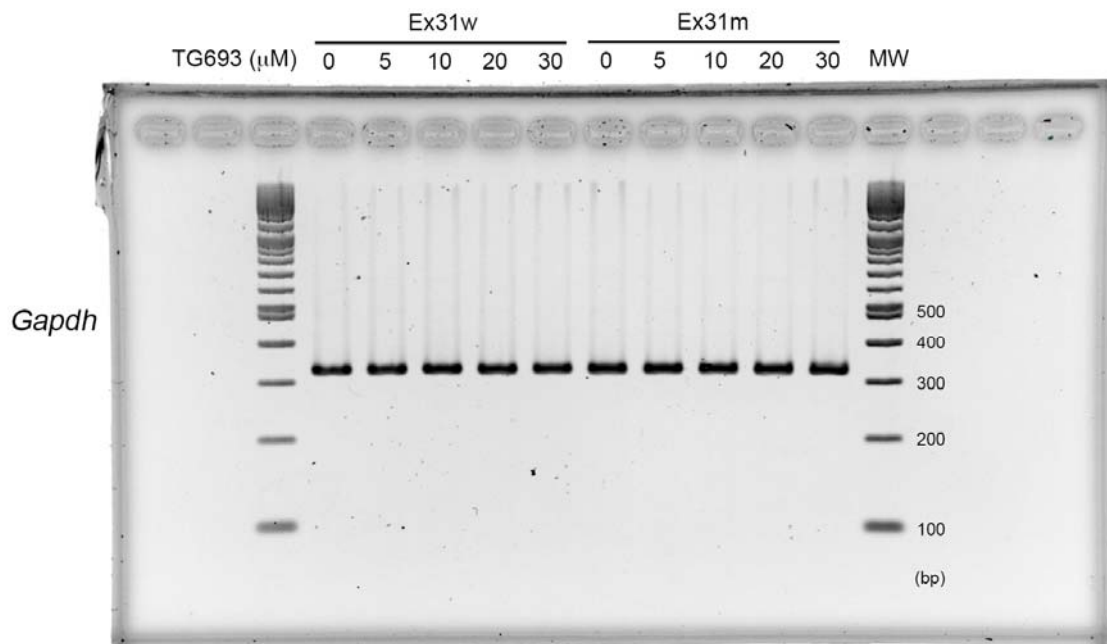
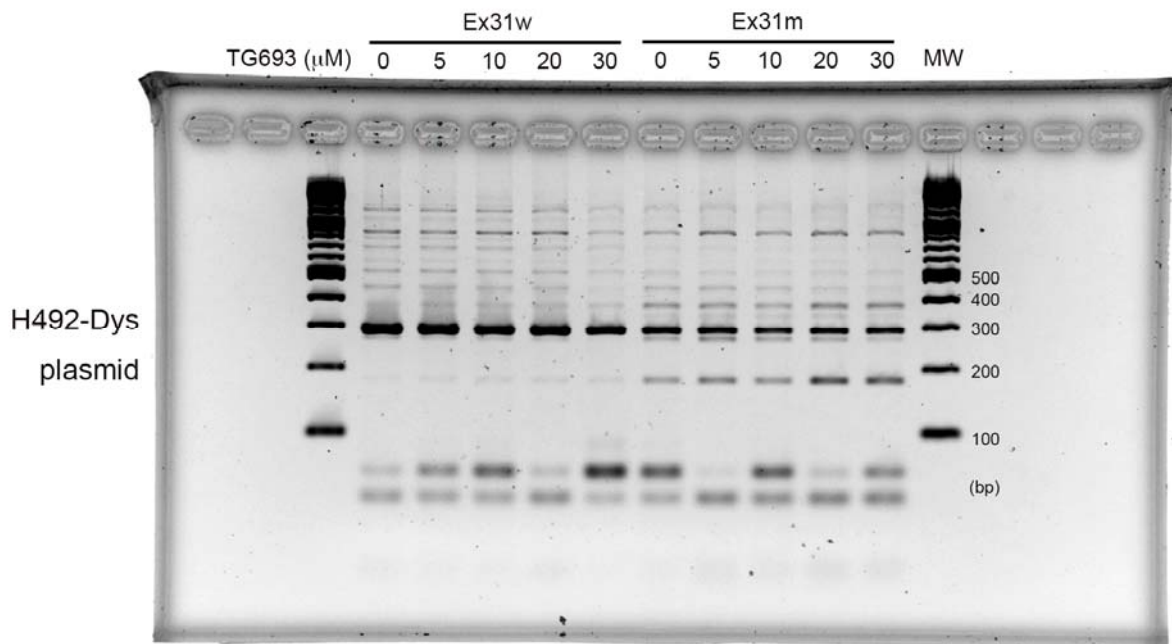
Body weight increased normally in male and female rats administrated orally with TG693 at dose of 100 mg kg⁻¹ for 7 days. Control animals were administrated the same amount of vehicle (0.5% methylcellulose) alone. Each value represents the mean and standard deviations (n=3). No mortality and no abnormalities in gross appearance of the animals were observed during the experimental period.



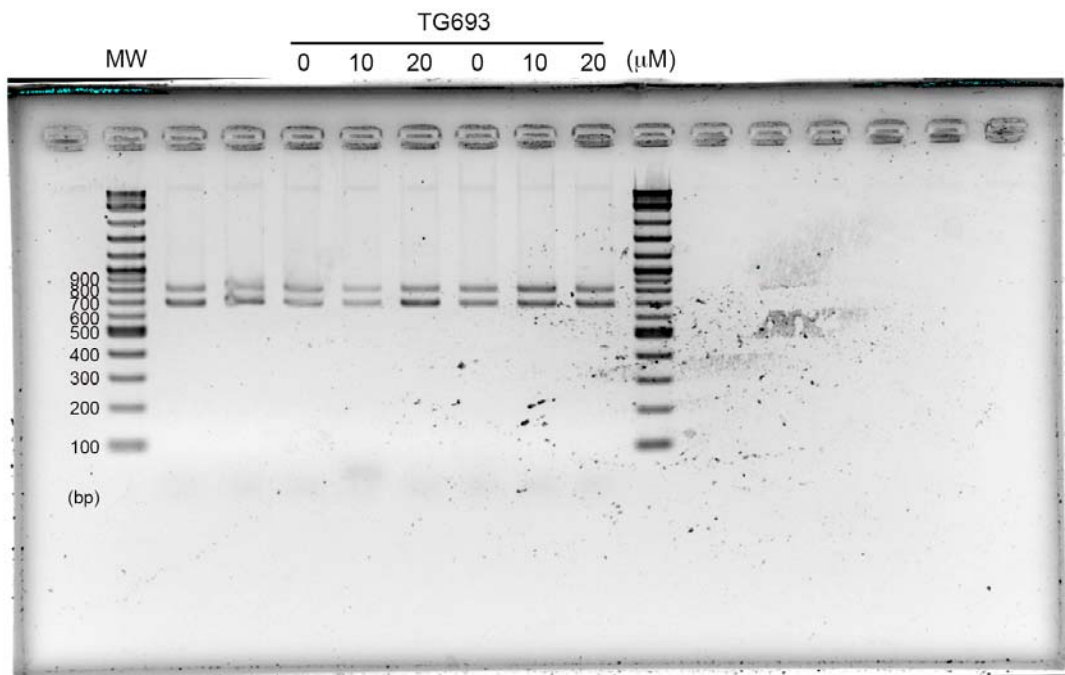
Supplementary figure S4. Full-length western blot images of Figure 2a



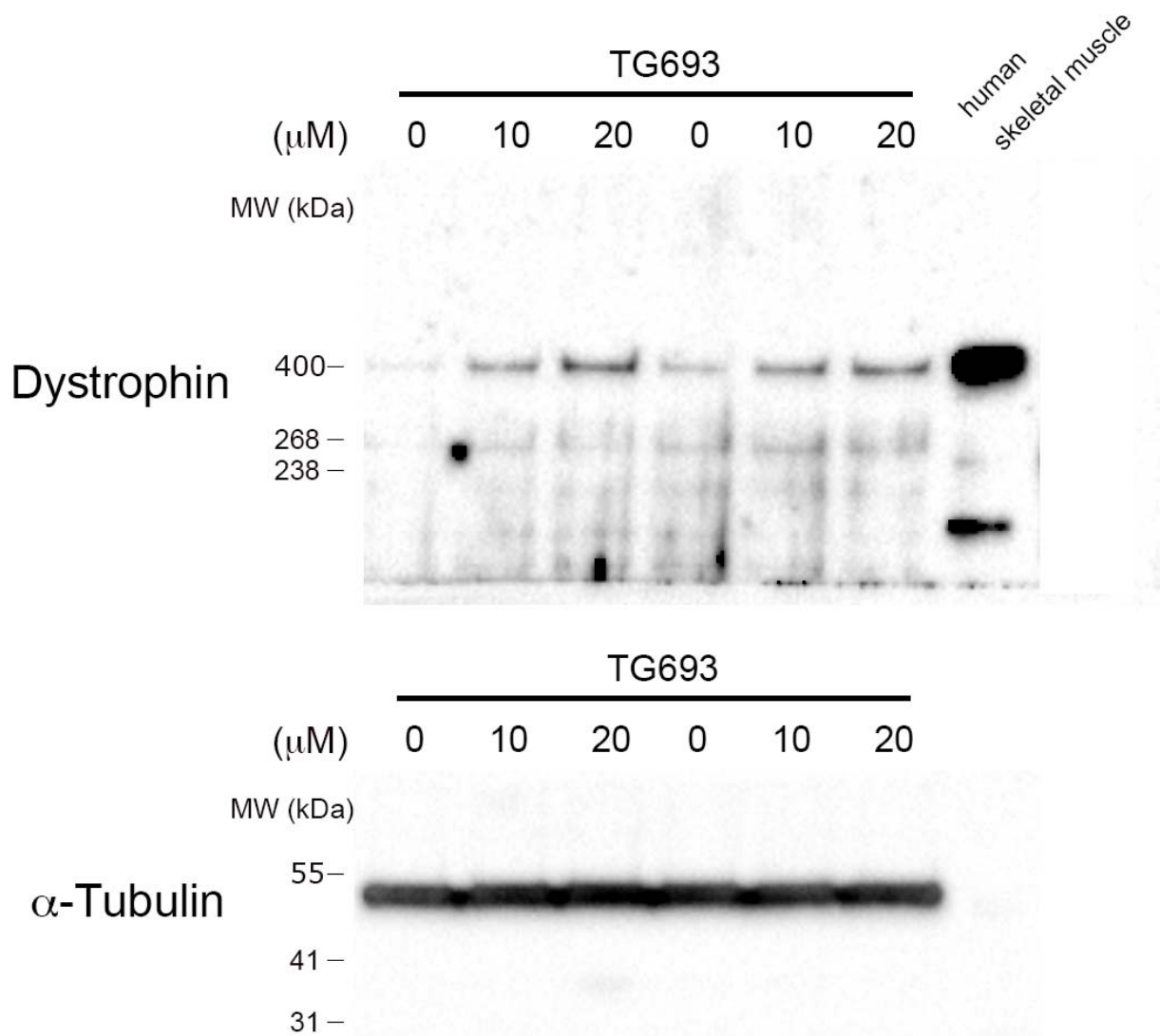
Supplementary figure S5. Agarose gel full images of Figure 2b



Supplementary figure S6. Agarose gel full images of Figure 2c

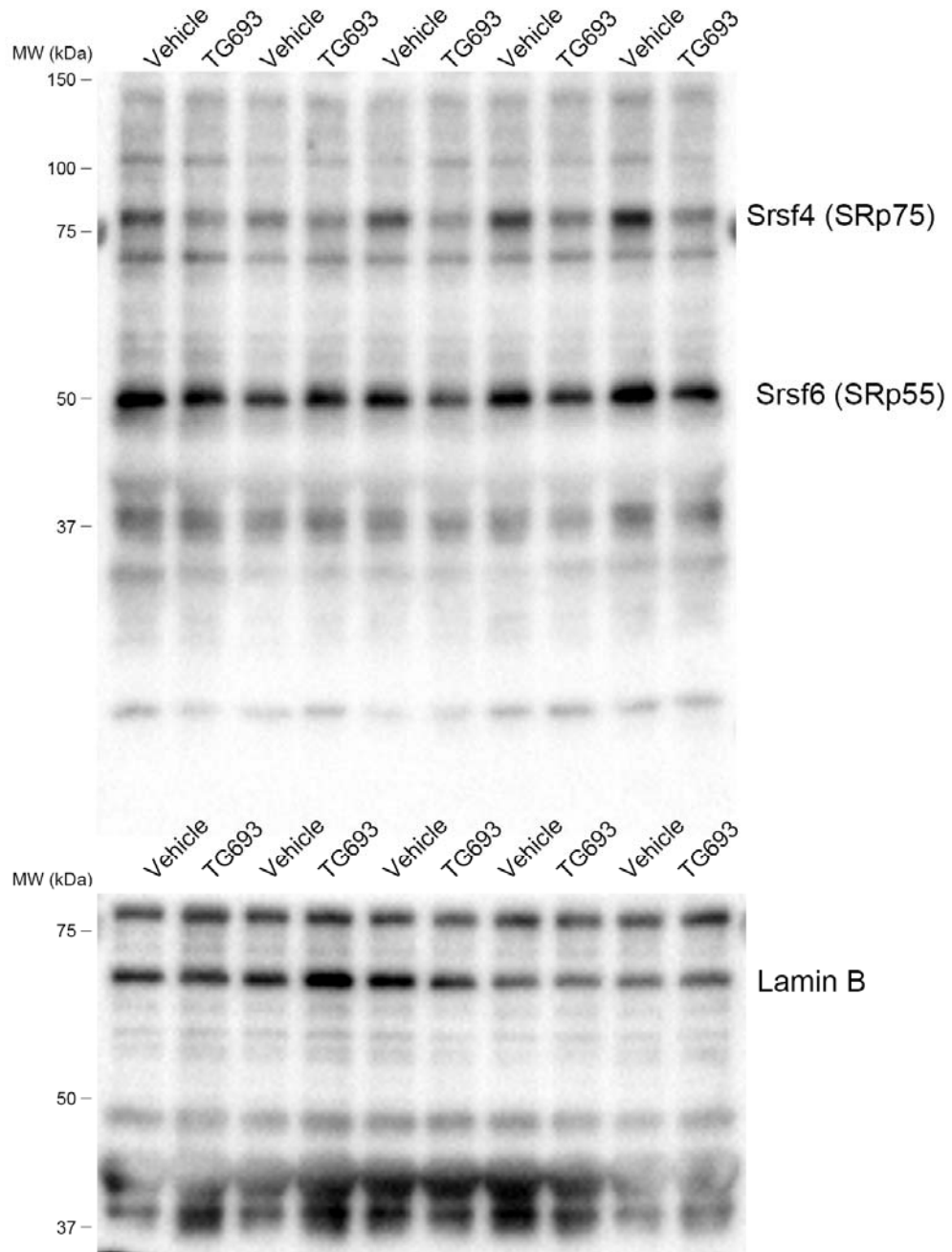


Supplementary figure S7. An agarose gel full image of Figure 3a

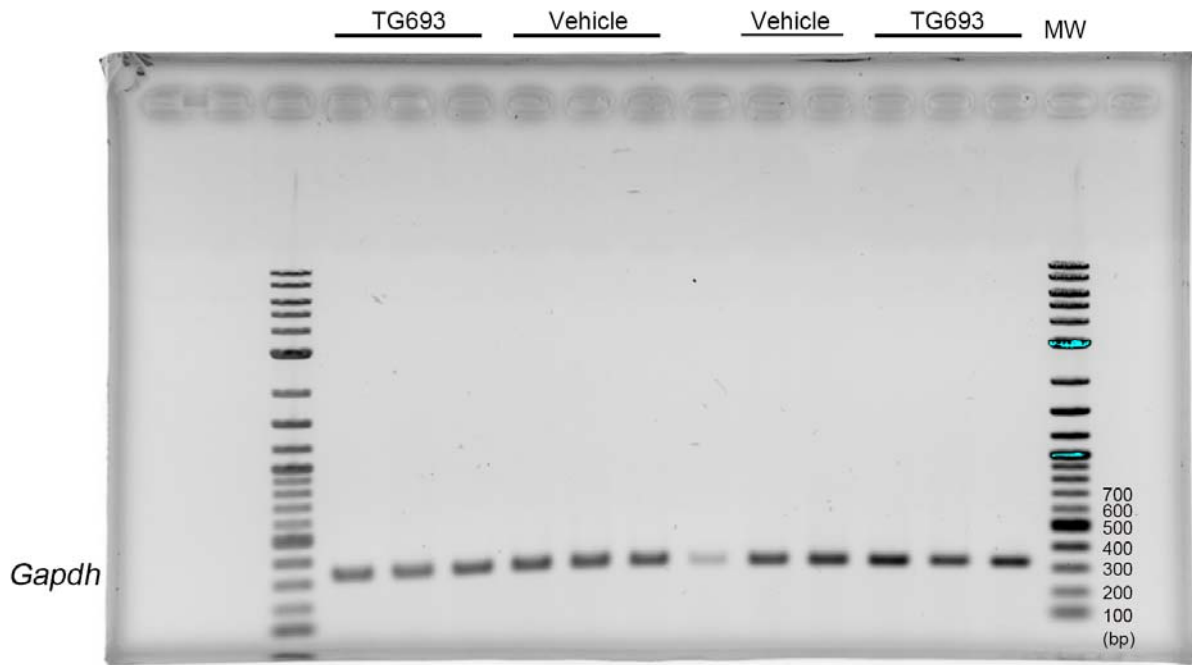
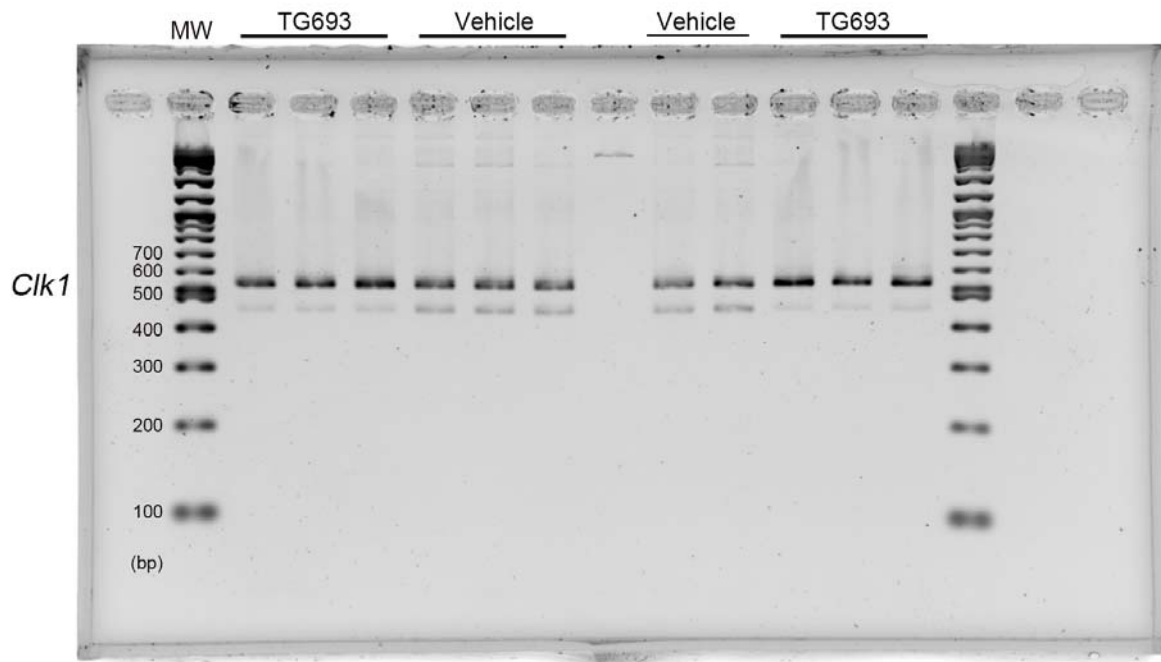


Supplementary figure S8. Full-length western blot images of Figure 3b

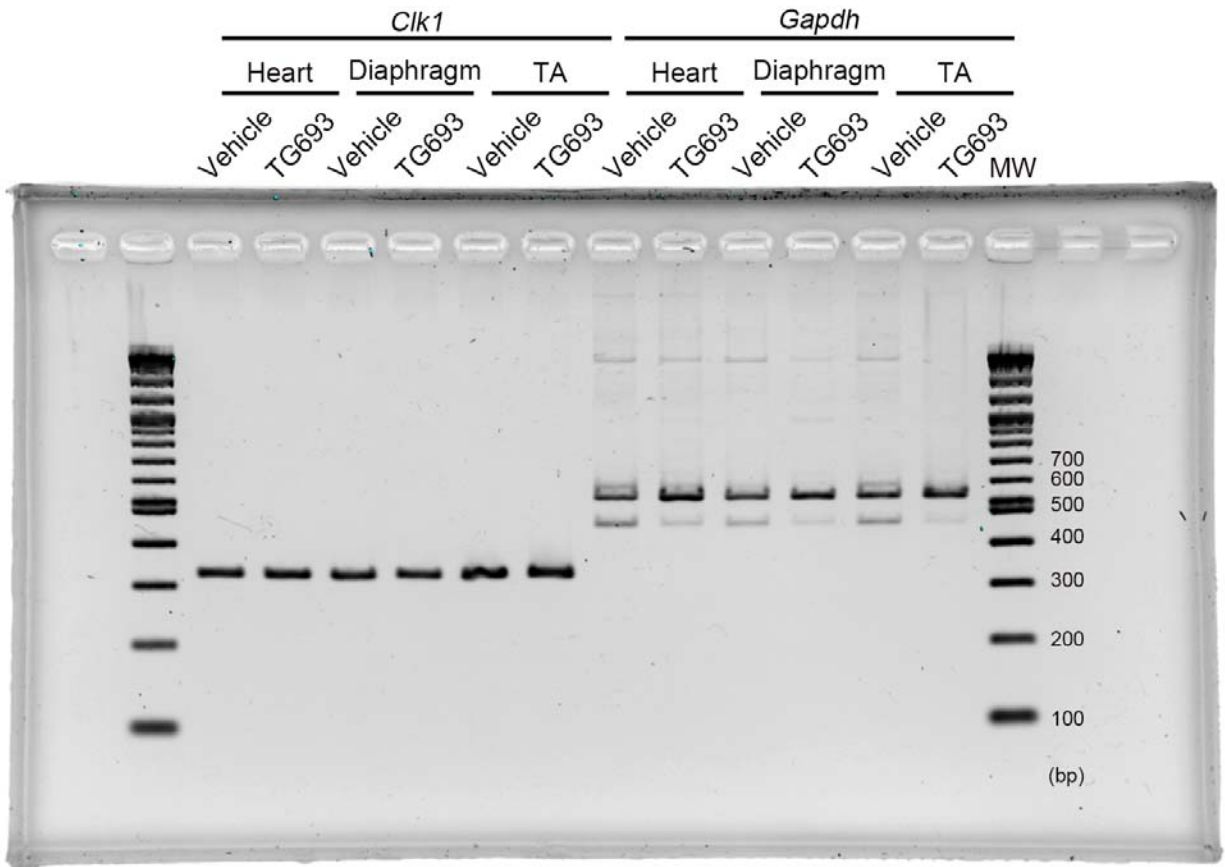
Skeletal Muscle (Human) Tissue Lysate (Cat.# ab29330, Abcam) was used as a positive control.



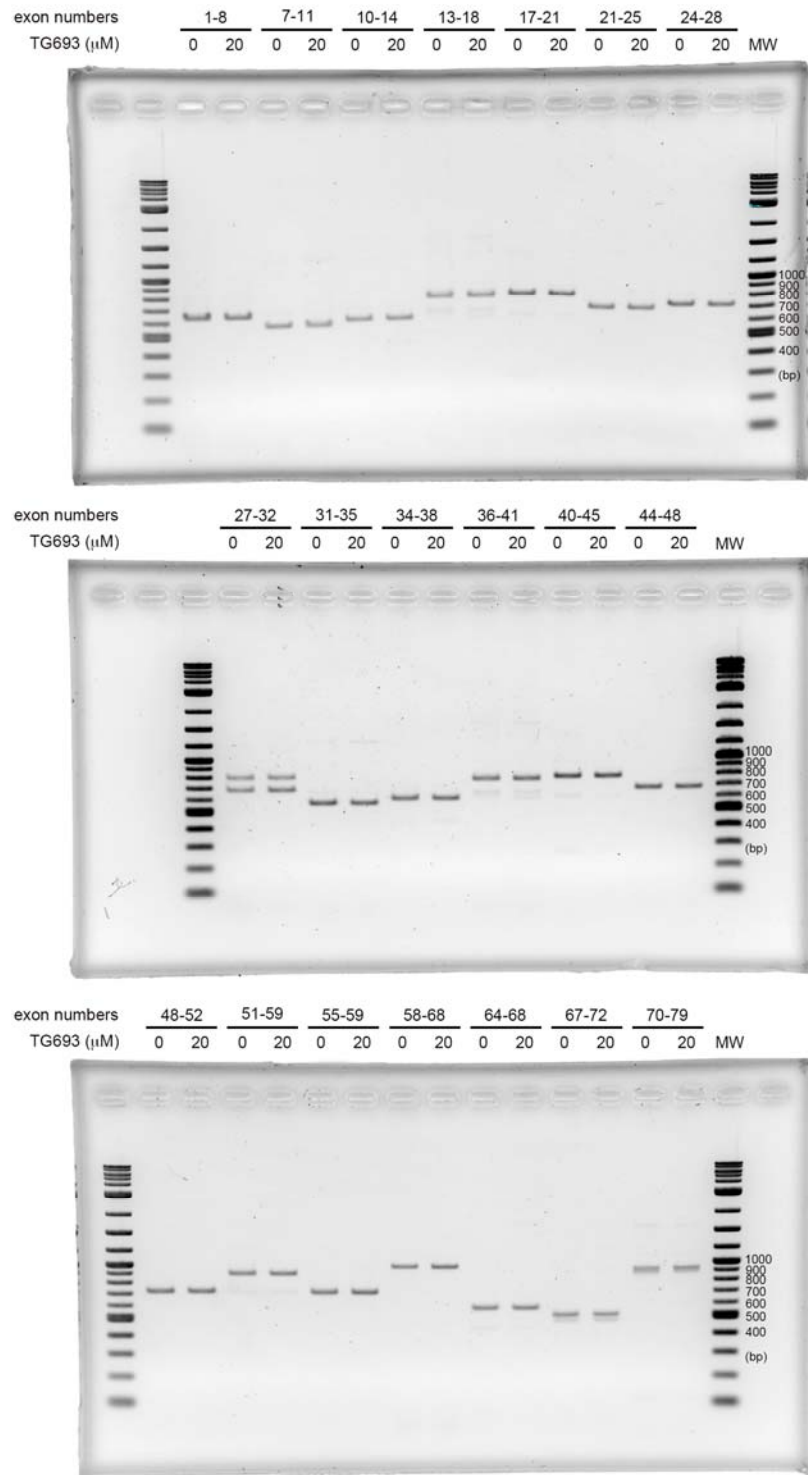
Supplementary figure S9. Full-length western blot images of Figure 4b



Supplementary figure S10. Agarose gel full images of Figure 4c



Supplementary figure S11. An agarose gel full image of Figure 4d



Supplementary figure S13. Agarose gel full images of Supplementary figure S2

Supporting Table

Table S1.

TG693 (nM)	K_m^{apparent} (μM)	$V_{max}^{\text{apparent}}$ (fmole/min)	alpha ^a	alpha' ^b
250	50.17 \pm 2.72	129.7 \pm 1.9	3.4	1.01
500	88.97 \pm 11.3	131.1 \pm 4.6	6.0	1.00
1000	142.8 \pm 16.13	121.8 \pm 4.1	10.3	1.07

Kinetic constants (\pm SEM) were estimated by fitting the data to the Michaelis-Menten equation.

^aAlpha is calculated by the following equation: $\alpha = (K_m^{\text{apparent}}/V_m^{\text{apparent}}) / (K_m/V_m)$

^bAlpha' is calculated by the following equation: $\alpha' = (1/V_m^{\text{apparent}}) / (1/V_m)$

These values indicated that TG693 ATP-competitively inhibits CLK1.

Table S2.

Average of two replicates is shown as percent inhibition of kinase activity in the presence of TG693 (1 μ M) relative to solvent control (DMSO).

CLK1 and Haspin were inhibited by over 90%.

Kinase	%Inhibition	Kinase	%Inhibition
ABL	-1.3	ABL(E255K)	-4.2
ABL(T315I)	6.5	ACK	-1.1
ALK	6.1	ALK(C1156Y)	0.1
ALK(F1174L)	-6.9	ALK(G1202R)	3.8
ALK(L1152insT)	-6.4	ALK(L1196M)	2.6
ALK(R1275Q)	-7.6	EML4-ALK	2.0
NPM1-ALK	3.0	ARG	4.7
AXL	3.5	BLK	-2.2
BMX	4.6	BRK	5.2
BTK	-9.5	CSK	-1.2
DDR1	-6.0	DDR2	-2.2
EGFR	-10.7	EGFR(d746-750)	0.6
EGFR(d746-750/T790M)	1.5	EGFR(L858R)	0.4
EGFR(L861Q)	-5.4	EGFR(T790M)	-0.2
EGFR(T790M/L858R)	1.3	EPHA1	-2.8
EPHA2	5.7	EPHA3	0.4
EPHA4	2.4	EPHA5	-7.5
EPHA6	-3.5	EPHA7	5.0
EPHA8	7.3	EPHB1	2.5
EPHB2	0.3	EPHB3	-0.5
EPHB4	-1.5	FAK	3.6
FER	4.4	FES	1.3

FGFR1	6.9	FGFR1(V561M)	-11.6
FGFR2	1.7	FGFR3	-0.6
FGFR3(K650E)	5.2	FGFR3(K650M)	7.8
FGFR4	4.3	FGFR4(V550E)	-4.1
FGFR4(V550L)	-36.6	FGR	-5.9
FLT1	5.9	FLT3	17.5
FLT4	-0.3	FMS	2.6
FRK	-2.3	FYN(isoform a)	-0.7
FYN(isoform b)	0.6	HCK	-3.0
HER2	-3.8	HER4	5.8
IGF1R	3.3	INSR	-5.9
IRR	3.0	ITK	2.8
JAK1	-0.7	JAK2	7.9
JAK3	11.6	KDR	0.1
KIT	-0.9	KIT(D816E)	-6.8
KIT(D816V)	-1.1	KIT(D816Y)	-1.7
KIT(T670D)	-0.7	KIT(V560G)	-2.6
KIT(V654A)	-1.5	LCK	-8.4
LTK	3.0	LYNa	0.1
LYNb	0.8	MER	3.0
MET	13.2	MET(D1228H)	0.6
MET(M1250T)	-0.8	MET(Y1235D)	-2.0
MUSK	-5.0	PDGFR α	6.2
PDGFR α (D842V)	0.8	PDGFR α (T674I)	7.6
PDGFR α (V561D)	2.7	PDGFR β	3.0
PYK2	3.3	RET	4.8
RET(G691S)	4.9	RET(M918T)	-2.6

RET(S891A)	-18.0	RET(Y791F)	3.0
RON	1.1	ROS	8.1
SRC	3.2	SRM	1.5
SYK	-60.9	TEC	-0.4
TIE2	9.7	TNK1	3.8
TRKA	5.1	TRKB	0.1
TRKC	7.7	TXK	-1.0
TYK2	0.6	TYRO3	0.3
YES	-9.6	YES(T348I)	-1.4
AKT1	-1.3	AKT2	-3.0
AKT3	-4.6	AMPK α 1/ β 1/ γ 1	-6.5
AMPK α 2/ β 1/ γ 1	1.7	AurA	-6.2
AurA/TPX2	8.5	AurB	6.1
AurC	2.5	BRAF_Cascade	-0.9
BRAF(V600E)_Cascade	7.9	BRSK1	1.1
BRSK2	6.7	CaMK1 α	1.5
CaMK1 δ	7.0	CaMK2 α	-3.3
CaMK2 β	2.8	CaMK2 γ	-2.4
CaMK2 δ	1.4	CaMK4	0.5
CDC2/CycB1	10.3	CDC7/ASK	10.8
CDK2/CycA2	41.4	CDK2/CycE1	18.1
CDK3/CycE1	11.4	CDK4/CycD3	5.4
CDK5/p25	21.8	CDK6/CycD3	9.1
CDK7/CycH/MAT1	6.2	CDK9/CycT1	57.8
CGK2	38.5	CHK1	1.7
CHK2	-1.0	CK1 α	11.9
CK1 γ 1	5.0	CK1 γ 2	-3.2

CK1 γ 3	-7.7	CK1 δ	21.3
CK1 ϵ	8.0	CK2 α 1/ β	3.5
CK2 α 2/ β	14.6	CLK1	92.6
CLK2	14.9	CLK3	11.7
COT_Cascade	1.4	CRIK	16.9
DAPK1	-1.8	DCAMKL2	9.6
DLK_Cascade	4.0	DYRK1A	84.3
DYRK1B	76.1	DYRK2	77.2
DYRK3	64.0	EEF2K	-15.2
Erk1	1.4	Erk2	-5.8
Erk5	2.2	GSK3 α	12.6
GSK3 β	8.5	Haspin	92.8
HGK	66.5	HIPK1	-3.5
HIPK2	-2.0	HIPK3	-0.7
HIPK4	7.6	IKK α	14.6
IKK β	14.6	IKK ϵ	6.1
IRAK1	4.2	IRAK4	8.4
JNK1	-18.0	JNK2	-5.9
JNK3	-4.4	LATS2	-3.8
LOK	5.9	MAP2K1_Cascade	-7.4
MAP2K2_Cascade	-4.2	MAP2K3_Cascade	0.0
MAP2K4_Cascade	-2.8	MAP2K5_Cascade	2.4
MAP2K6_Cascade	3.8	MAP2K7_Cascade	0.6
MAP3K1_Cascade	-5.0	MAP3K2_Cascade	3.4
MAP3K3_Cascade	7.5	MAP3K4_Cascade	-0.7
MAP3K5_Cascade	3.1	MAP4K2	1.9
MAPKAPK2	-26.0	MAPKAPK3	-13.1

MAPKAPK5	2.6	MARK1	13.3
MARK2	20.3	MARK3	15.5
MARK4	25.1	MELK	5.7
MGC42105	-22.2	MINK	23.2
MLK1_Cascade	-1.6	MLK2_Cascade	-4.5
MLK3_Cascade	-1.6	MNK1	45.7
MNK2	57.3	MOS_Cascade	-5.2
MRCK α	-18.2	MRCK β	-7.3
MSK1	1.2	MSK2	-5.1
MSSK1	-7.3	MST1	-1.9
MST2	0.5	MST3	1.0
MST4	4.1	NDR1	11.5
NDR2	7.5	NEK1	-1.5
NEK2	-11.9	NEK4	-4.2
NEK6	-2.5	NEK7	-9.0
NEK9	-5.1	NuaK1	7.5
NuaK2	0.4	p38 α	-0.1
p38 β	-1.5	p38 γ	1.4
p38 δ	-0.7	p70S6K	46.0
p70S6K β	18.7	PAK1	-3.8
PAK2	-51.3	PAK4	-13.7
PAK5	-14.0	PAK6	-4.3
PASK	14.7	PBK	-3.5
PDHK2	-0.8	PDHK4	3.1
PDK1	-3.9	PEK	5.0
PGK	11.0	PHKG1	0.0
PHKG2	6.3	PIM1	1.2

PIM2	-3.5	PIM3	6.6
PKAC α	9.5	PKAC β	3.1
PKAC γ	1.5	PKC α	-5.4
PKC β 1	-11.4	PKC β 2	-11.8
PKC γ	-11.4	PKC δ	1.5
PKC ϵ	12.3	PKC ζ	-9.7
PKC η	5.8	PKC θ	-12.6
PKC ι	-6.8	PKD1	-15.8
PKD2	5.4	PKD3	-9.0
PKN1	34.5	PKR	1.2
PLK1	-8.5	PLK2	2.9
PLK3	1.7	PRKX	12.2
QIK	3.4	RAF1_Cascade	-5.1
ROCK1	27.6	ROCK2	46.3
RSK1	-4.7	RSK2	2.1
RSK3	-4.8	RSK4	-6.5
SGK	5.6	SGK2	-5.4
SGK3	-3.2	SIK	3.2
skMLCK	0.9	SLK	1.2
SRPK1	0.6	SRPK2	0.5
TAK1-TAB1_Cascade	2.9	TAOK2	2.0
TBK1	5.8	TNIK	48.6
TSSK1	3.0	TSSK2	-0.1
TSSK3	0.8	WNK1	4.1
WNK2	4.0	WNK3	-4.9
PIK3CA/PIK3R1	36.8	SPHK1	-2.3
SPHK2	4.1		

Table S3.

The commercially available antibodies used in this study.

Antibody		Clone ID	Vendor	Cat. No.
SR proteins	rmouse monoclonal	1H4	Thermo Fisher Scientific	33-9400
α -Tubullin	rmouse monoclonal	DM1A	Thermo Fisher Scientific	MS-581-P1
Dystrophin	rabbit polyclonal		Abcam	ab15277
Lamin B	goat polyclonal	M-20	Santa Cruz Biotechnology	sc-6217

Table S4.

Primers used to investigate splicing of all dystrophin introns in patient-derived cells

(Supplementary figure S3)

Exons amplified	Location	Sequence
1-8	1-22	ATGCTTTGGTGGGAAGAAGTAG
1-8	831-809	CTGTTGAGAATAGTGCATTTGAT
7-11	556-579	GTGGTTTGCCAGCAGTCAGCCACA
7-11	1230-108	TCCTGTTCCAATCAGCTTACTTC
10-14	1084-1104	TTGCAAGCACAAGGAGAGATT
10-14	1689-1669	ACGTTGCCATTTGAGAAGGAT
13-18	1579-1599	GCTGCTTTGGAAGAACA ACTT
13-18	2218-2197	CTTCTGAGCGAGTAATCCAGCT
17-21	2134-2156	AGGCAGATTACTGTGGATTCTGA
17-21	2803-2783	TTGTCTGTAGCTCTTTCTCTC
21-25	2650-2669	CAACCTCAAATTGAACGATT
21-25	3336-3316	CCCACCTTCATTGACACTGTT
24-28	3112-3134	GAGCATTGTCAAAGCTAGAGGA
24-28	3816-3793	CAATAACTCATGCCAACATGCCCA
27-32	3688-3708	CCTGTAGCACAAGAGGCCTTA
27-32	4481-4460	TCCACACTCTTTGTTTCCAATG
31-35	4309-4328	GCCCAAAGAGTCCTGTCTCA
31-35	4881-4862	GTGCACCTTCTGTTTCTCAA
34-38	4753-4772	GAATGGCTGGCAGCTACAGA
34-38	5360-5338	TTAAACTGCTCCAATTCCTTCAA
36-41	5050-5069	TTTGACCAGAATGTGGACCA
36-41	5826-5806	TGCGGCCCATCCTCAGACAA
40-45	5704-5725	AGCCTACCTGAGCCCAGAGATG

40-45	6502-6483	CTTCCCCAGTTGCATTCAAT
44-48	6367-6393	GCTGAACAGTTTCTCAGAAAGACACAA
44-48	7053-7033	CAACTGATTCCTAATAGGAGA
48-52	6937-6957	CAAGGAGAAATTGAAGCTCAA
48-52	7658-7636	CGATCCGTAATGATTGTTCTAGC
51-59	7435-7455	TGGACAGAACTTACCGACTGG
51-59	8326-8307	GTAACAGGACTGCATCATCG
55-59	8040-8059	AGAGGCTGCTTTGGAAGAAA
55-59	8746-8725	CCCCTCAGTATTGACCTCCTC
58-68	8619-8638	GACAGAGCAGCCTTTGGAAG
58-68	9589-9568	GGACACGGATCCTCCCTGTTCG
64-68	9334-9353	CTCCGAAGACTGCAGAAGGC
64-68	9916-9898	TTTCTGCAGCAGCCACTCT
67-72	9775-9792	ATTGAGCCAAGTGTCCGG
67-72	10297-10277	TATCATCGTGTGAAAGCTGAG
70-79	10107-10127	GAATGGGCTACCTGCCAGTG
70-79	11162-11142	ATCGCTCTGCCCAAATCATCTG

Table S5.

Reaction conditions for each kinase (Figure 1e and Supplementary Table S1)

Kinase	Platform	Substrate		ATP (μ M)		Metal	
		Name	(nM)	Km	Assay	Name	(mM)
ABL	MSA	ABLtide	1000	16	25	Mg	5
ABL[E255K]	MSA	ABLtide	1000	17	25	Mg	5
ABL[T315I]	MSA	ABLtide	1000	4	5	Mg	5
ACK ¹⁾	MSA	WASP peptide	1000	97	100	Mg	5
ALK	MSA	Srctide	1000	57	50	Mg	5
ALK[C1156Y]	MSA	Srctide	1000	64	75	Mg	5
ALK[F1174L]	MSA	Srctide	1000	49	50	Mg	5
ALK[G1202R]	MSA	Srctide	1000	31	50	Mg	5
ALK[L1152insT]	MSA	Srctide	1000	108	100	Mg	5
ALK[L1196M]	MSA	Srctide	1000	57	75	Mg	5
ALK[R1275Q]	MSA	Srctide	1000	84	100	Mg	5
EML4-ALK ¹⁾	MSA	Srctide	1000	43	50	Mg	5
NPM1-ALK	MSA	Srctide	1000	57	50	Mg	5
ARG	MSA	ABLtide	1000	24	25	Mg	5
AXL	MSA	CSKtide	1000	32	50	Mg	5
BLK	MSA	Srctide	1000	62	75	Mg	5
BMX	MSA	Srctide	1000	75	75	Mg	5
BRK ¹⁾	MSA	Blk/Lyntide	1000	250	250	Mg	5
BTK	MSA	Srctide	1000	72	75	Mg	5
CSK ¹⁾	MSA	Srctide	1000	4.8	5	Mg+Mn	5+1
DDR1 ¹⁾	MSA	IRS1	1000	94	100	Mg	5
DDR2 ¹⁾	MSA	IRS1	1000	38	50	Mg	5
EGFR	MSA	Srctide	1000	2.7	5	Mg+Mn	5+1

EGFR[d746-750]	MSA	Srctide	1000	19	25	Mg+Mn	5+1
EGFR[d746-750/ T790M]	MSA	Srctide	1000	5.4	5	Mg+Mn	5+1
EGFR[L858R]	MSA	Srctide	1000	9.8	10	Mg+Mn	5+1
EGFR[L861Q]	MSA	Srctide	1000	7.5	10	Mg+Mn	5+1
EGFR[T790M]	MSA	Srctide	1000	0.9	1	Mg+Mn	5+1
EGFR[T790M/L858R]	MSA	Srctide	1000	1.9	2	Mg+Mn	5+1
EPHA1	MSA	Blk/Lyntide	1000	22	25	Mg	5
EPHA2	MSA	Blk/Lyntide	1000	67	75	Mg	5
EPHA3	MSA	Blk/Lyntide	1000	170	150	Mg	5
EPHA4	MSA	Blk/Lyntide	1000	52	50	Mg	5
EPHA5	MSA	Blk/Lyntide	1000	56	50	Mg	5
EPHA6	MSA	Blk/Lyntide	1000	27	25	Mg	5
EPHA7	MSA	Blk/Lyntide	1000	58	50	Mg	5
EPHA8	MSA	Blk/Lyntide	1000	69	75	Mg	5
EPHB1	MSA	Blk/Lyntide	1000	29	25	Mg	5
EPHB2	MSA	Blk/Lyntide	1000	86	100	Mg	5
EPHB3	MSA	Blk/Lyntide	1000	49	50	Mg	5
EPHB4	MSA	Blk/Lyntide	1000	56	50	Mg	5
FAK ¹⁾	MSA	Blk/Lyntide	1000	25	25	Mg	5
FER	MSA	Srctide	1000	26	25	Mg	5
FES	MSA	Srctide	1000	43	50	Mg	5
FGFR1	MSA	CSKtide	1000	89	100	Mg	5
FGFR1[V561M]	MSA	CSKtide	1000	33	50	Mg	5
FGFR2	MSA	CSKtide	1000	66	75	Mg	5
FGFR3	MSA	CSKtide	1000	43	50	Mg	5
FGFR3[K650E]	MSA	CSKtide	1000	41	50	Mg	5

FGFR3[K650M]	MSA	CSKtide	1000	17	25	Mg	5
FGFR4	MSA	CSKtide	1000	230	250	Mg	5
FGFR4[V550E]	MSA	CSKtide	1000	210	200	Mg	5
FGFR4[V550L]	MSA	CSKtide	1000	160	150	Mg	5
FGR	MSA	Srctide	1000	34	50	Mg	5
FLT1	MSA	CSKtide	1000	140	150	Mg	5
FLT3	MSA	Srctide	1000	94	100	Mg	5
FLT4	MSA	CSKtide	1000	72	75	Mg	5
FMS	MSA	Srctide	1000	26	25	Mg	5
FRK	MSA	Srctide	1000	62	75	Mg	5
FYN[isoform a]	MSA	Srctide	1000	36	50	Mg	5
FYN[isoform b]	MSA	Srctide	1000	20	25	Mg	5
HCK	MSA	Srctide	1000	11	10	Mg	5
HER2	MSA	Srctide	1000	9.4	10	Mn	5
HER4	MSA	Srctide	1000	27	25	Mg	5
IGF1R	MSA	IRS1	1000	63	75	Mg	5
INSR	MSA	IRS1	1000	58	50	Mg	5
IRR	MSA	IRS1	1000	64	75	Mg	5
ITK	MSA	Srctide	1000	6.1	10	Mg	5
JAK1 ¹⁵⁾	MSA	JAK1 substrate peptide	1000	68	75	Mg	5
JAK2	MSA	Srctide	1000	13	10	Mg	5
JAK3	MSA	Srctide	1000	3.5	5	Mg	5
KDR	MSA	CSKtide	1000	74	75	Mg	5
KIT ⁵⁾	MSA	Srctide	1000	370	400	Mg	5
KIT[D816E] ⁵⁾	MSA	Srctide	1000	40	50	Mg	5
KIT[D816V] ⁵⁾	MSA	Srctide	1000	14	10	Mg	5

KIT[D816Y] ⁵⁾	MSA	Srctide	1000	22	25	Mg	5
KIT[T670I] ⁵⁾	MSA	Srctide	1000	100	100	Mg	5
KIT[V560G] ⁵⁾	MSA	Srctide	1000	110	250	Mg	5
KIT[V654A] ⁵⁾	MSA	Srctide	1000	220	250	Mg	5
LCK	MSA	Srctide	1000	14	10	Mg	5
LTK	MSA	Srctide	1000	49	50	Mg	5
LYNa	MSA	Srctide	1000	14	10	Mg	5
LYNb	MSA	Srctide	1000	18	25	Mg	5
MER	MSA	CSKtide	1000	36	50	Mg	5
MET	MSA	Srctide	1000	27	25	Mg	5
MET[D1228H]	MSA	Srctide	1000	25	25	Mg	5
MET[M1250T]	MSA	Srctide	1000	17	25	Mg	5
MET[Y1235D]	MSA	Srctide	1000	71	75	Mg	5
MUSK ¹⁾	MSA	CSKtide	1000	14	10	Mg+Mn	5+1
PDGFR α	MSA	CSKtide	1000	28	25	Mg	5
PDGFR α [D842V]	MSA	CSKtide	1000	21	25	Mg	5
PDGFR α [T674I] ¹⁾	MSA	CSKtide	1000	11	10	Mg	5
PDGFR α [V561D]	MSA	CSKtide	1000	35	50	Mg	5
PDGFR β	MSA	CSKtide	1000	23	25	Mg	5
PYK2	MSA	Blk/Lyntide	1000	56	50	Mg	5
RET	MSA	CSKtide	1000	7.5	10	Mg	5
RET[G691S]	MSA	CSKtide	1000	13	10	Mg	5
RET[M918T]	MSA	CSKtide	1000	4.2	5	Mg	5
RET[S891A]	MSA	CSKtide	1000	11	10	Mg	5
RET[Y791F]	MSA	CSKtide	1000	29	25	Mg	5
RON	MSA	Srctide	1000	27	25	Mg	5
ROS	MSA	IRS1	1000	37	50	Mg	5

SRC	MSA	Srctide	1000	31	50	Mg	5
SRM	MSA	Blk/Lyntide	1000	38	50	Mg	5
SYK	MSA	Blk/Lyntide	1000	26	25	Mg	5
TEC	MSA	Srctide	1000	55	50	Mg	5
TIE2	MSA	Blk/Lyntide	1000	94	100	Mg	5
TNK1 ¹⁾	MSA	CSKtide	1000	71	75	Mg	5
TRKA	MSA	CSKtide	1000	65	75	Mg	5
TRKB	MSA	Srctide	1000	80	75	Mg	5
TRKC	MSA	Srctide	1000	47	50	Mg	5
TXK ¹⁾	MSA	Srctide	1000	110	100	Mg	5
TYK2 ¹⁾	MSA	Srctide	1000	18	25	Mg	5
TYRO3	MSA	CSKtide	1000	80	75	Mg	5
YES	MSA	Srctide	1000	13	10	Mg	5
YES[T348I]	MSA	Srctide	1000	8.5	10	Mg	5
AKT1	MSA	Crosstide	1000	31	50	Mg	5
AKT2	MSA	Crosstide	1000	110	100	Mg	5
AKT3	MSA	Crosstide	1000	54	50	Mg	5
AMPK α 1/ β 1/ γ 1	MSA	SAMS peptide	1000	130	150	Mg	5
AMPK α 2/ β 1/ γ 1	MSA	SAMS peptide	1000	100	100	Mg	5
AurA	MSA	Kemptide	1000	27	25	Mg	5
AurA/TPX2 ⁹⁾	MSA	Kemptide	1000	1.7	2	Mg	5
AurB/INCENP	MSA	Kemptide	1000	16	25	Mg	5
AurC	MSA	Kemptide	1000	24	25	Mg	5
BRAF_Cascade	MSA	MAP2K1	1	-	1000	Mg	5
		Erk2	2.5				
		Modified Erktide	1000				
BRAF[V600E]_Cascade	MSA	MAP2K1	1	-	1000	Mg	5

		Erk2	2.5				
		Modified Erktide	1000				
BRSK1	MSA	CHKtide	1000	30	25	Mg	5
BRSK2	MSA	CHKtide	1000	31	50	Mg	5
CaMK1 α ¹⁾²⁾	MSA	GS peptide	1000	750	1000	Mg	5
CaMK1 δ ¹⁾²⁾	MSA	Synapsin peptide	1000	11	10	Mg	5
CaMK2 α ²⁾	MSA	GS peptide	1000	33	50	Mg	5
CaMK2 β ²⁾	MSA	GS peptide	1000	19	25	Mg	5
CaMK2 γ ²⁾	MSA	GS peptide	1000	23	25	Mg	5
CaMK2 δ ²⁾	MSA	GS peptide	1000	6.3	5	Mg	5
CaMK4 ²⁾	MSA	GS peptide	1000	20	25	Mg	5
CDC2/CycB1	MSA	Modified Histone H1	1000	34	50	Mg	5
CDC7/ASK ¹⁾	MSA	MCM2 peptide	1000	2.8	5	Mg	10
CDK2/CycA2	MSA	Modified Histone H1	1000	27	25	Mg	5
CDK2/CycE1	MSA	Modified Histone H1	1000	130	150	Mg	5
CDK3/CycE1	MSA	Modified Histone H1	1000	1000	1000	Mg	5
CDK4/CycD3 ¹⁾	MSA	DYRKtide-F	1000	200	200	Mg	5
CDK5/p25	MSA	Modified Histone H1	1000	10	10	Mg	5
CDK6/CycD3 ¹⁾	MSA	DYRKtide-F	1000	330	300	Mg	5
CDK7/CycH/MAT1 ¹⁾	MSA	CTD3 peptide	1000	32	50	Mg	5
CDK9/CycT1 ¹⁾	MSA	CDK9 substrate	1000	9.4	10	Mg	5
CGK2 ³⁾	MSA	Kemptide	1000	24	25	Mg	5

CHK1	MSA	CHKtide	1000	50	50	Mg	5
CHK2	MSA	CHKtide	1000	51	50	Mg	5
CK1 α ¹⁾	MSA	CKtide	1000	4.1	5	Mg	5
CK1 γ 1	MSA	CKtide	1000	6.3	5	Mg	5
CK1 γ 2	MSA	CKtide	1000	10	10	Mg	5
CK1 γ 3	MSA	CKtide	1000	3.2	5	Mg	5
CK1 δ	MSA	CKtide	1000	7.7	10	Mg	5
CK1 ϵ ¹⁾	MSA	CKtide	1000	16	25	Mg	5
CK2 α 1/ β	MSA	CK2tide	1000	2.9	5	Mg	5
CK2 α 2/ β	MSA	CK2tide	1000	2.1	5	Mg	5
CLK1	MSA	DYRKtide-F	1000	11	10	Mg	5
CLK2	MSA	DYRKtide-F	1000	140	150	Mg	5
CLK3	MSA	DYRKtide-F	1000	75	75	Mg	5
COT_Cascade	MSA	MAP2K1	1	-	1000	Mg	5
		Erk2	2.5				
		Modified Erktide	1000				
CRIK ¹⁾	MSA	Histone H3 peptide	1000	7.8	10	Mg	5
DAPK1	MSA	DAPK1tide	1000	1.1	1	Mg	5
DCAMKL2 ¹⁾	MSA	GS peptide	1000	120	150	Mg	5
DLK_Cascade ¹⁾	MSA	MAP2K4 / MAP2K7	0.5 / 0.5	-	1000	Mg	5
		JNK2	50				
		Modified Erktide	1000				
DYRK1A	MSA	DYRKtide-F	1000	16	25	Mg	5
DYRK1B	MSA	DYRKtide-F	1000	59	50	Mg	5
DYRK2	MSA	DYRKtide-F	1000	7.7	10	Mg	5
DYRK3	MSA	DYRKtide-F	1000	6.8	5	Mg	5

EEF2K ¹⁾²⁾	MSA	EEF2Ktide	1000	12	10	Mg	5
Erk1	MSA	Modified Erktide	1000	34	50	Mg	5
Erk2	MSA	Modified Erktide	1000	33	50	Mg	5
Erk5 ¹⁾	MSA	EGFR-derived peptide	1000	450	1000	Mg	5
GSK3 α	MSA	CREBtide-p	1000	12	10	Mg	5
GSK3 β	MSA	CREBtide-p	1000	9.1	10	Mg	5
Haspin	MSA	Histone H3 peptide	1000	140	150	Mg	5
HGK	MSA	Moesin-derived peptide	1000	9.4	10	Mg	5
HIPK1	MSA	DYRKtide-F	1000	4.4	5	Mg	5
HIPK2	MSA	DYRKtide-F	1000	5.9	5	Mg	5
HIPK3	MSA	DYRKtide-F	1000	7.3	5	Mg	5
HIPK4	MSA	DYRKtide-F	1000	7	5	Mg	5
IKK α	IMAP	I κ B α peptide	100	41	40	Mg	10
IKK β	MSA	Modified I κ B α -derived peptide	1000	16	25	Mg	5
IKK ϵ ¹⁾	MSA	I κ B α peptide	1000	9.5	10	Mg	5
IRAK1	IMAP	SRPKtide	100	27	25	Mg	2.5
IRAK4 ¹⁾	MSA	IRAK1 peptide	1000	917	1000	Mg	5
JNK1	MSA	Modified Erktide	1000	29	100	Mg	5
JNK2	MSA	Modified Erktide	1000	21	50	Mg	5
JNK3	MSA	Modified Erktide	1000	6	25	Mg	5
LATS2 ¹⁾	MSA	SGKtide	1000	380	400	Mg	5
LOK ¹⁾	MSA	Moesin-derived peptide	1000	100	100	Mg	5
MAP2K1_Cascade	MSA	Erk2	2.5	-	1000	Mg	5

		Modified Erktide	1000				
MAP2K2_Cascade	MSA	Erk2	2.5	-	1000	Mg	5
		Modified Erktide	1000				
MAP2K3_Cascade	MSA	p38 α (9-352)	10	-	1000	Mg	5
		Modified Erktide	1000				
MAP2K4_Cascade ¹⁾	MSA	JNK2	50	-	1000	Mg	5
		Modified Erktide	1000				
MAP2K5_Cascade ¹⁾	MSA	Erk5	50	-	1000	Mg	5
		EGFR-derived peptide	1000				
MAP2K6_Cascade	MSA	p38 α (9-352)	10	-	1000	Mg	5
		Modified Erktide	1000				
MAP2K7_Cascade ¹⁾	MSA	JNK2	50	-	1000	Mg	5
		Modified Erktide	1000				
MAP3K1_Cascade	MSA	MAP2K1	1	-	1000	Mg	5
		Erk2	2.5				
		Modified Erktide	1000				
MAP3K2_Cascade ¹⁾	MSA	MAP2K4 /	0.5 /	-	1000	Mg	5
		MAP2K7	0.5				
		JNK2	50				
		Modified Erktide	1000				
MAP3K3_Cascade	MSA	MAP2K6	1	-	1000	Mg	5
		p38 α (9-352)	10				
		Modified Erktide	1000				
MAP3K4_Cascade	MSA	MAP2K6	1	-	1000	Mg	5
		p38 α (9-352)	10				
		Modified Erktide	1000				

MAP3K5_Cascade	MSA	MAP2K6	1	-	1000	Mg	5
		p38 α (9-352)	10				
		Modified Erktide	1000				
MAP4K2	MSA	S6k2 peptide	1000	93	100	Mg	5
MAPKAPK2	MSA	GS peptide	1000	3.6	5	Mg	5
MAPKAPK3	MSA	GS peptide	1000	13	10	Mg	5
MAPKAPK5	MSA	GS peptide	1000	12	10	Mg	5
MARK1	MSA	CHKtide	1000	8	10	Mg	5
MARK2	MSA	CHKtide	1000	8.8	10	Mg	5
MARK3	MSA	CHKtide	1000	5	5	Mg	5
MARK4	MSA	CHKtide	1000	12	10	Mg	5
MELK ¹⁾	MSA	GS peptide	1000	38	50	Mg	5
MGC42105	MSA	CHKtide	1000	21	25	Mg	5
MINK ¹⁾	MSA	Modified Erktide	1000	36	50	Mg	5
MLK1_Cascade	MSA	MAP2K1	1	-	1000	Mg	5
		Erk2	2.5				
		Modified Erktide	1000				
MLK2_Cascade	MSA	MAP2K1	1	-	1000	Mg	5
		Erk2	2.5				
		Modified Erktide	1000				
MLK3_Cascade	MSA	MAP2K1	1	-	1000	Mg	5
		Erk2	2.5				
		Modified Erktide	1000				
MNK1	MSA	RS peptide	1000	460	450	Mg	5
MNK2	MSA	RS peptide	1000	110	100	Mg	5
MOS_Cascade	MSA	MAP2K1	1	-	1000	Mg	5
		Erk2	2.5				

		Modified Erktide	1000				
MRCK α ¹⁾	MSA	DAPK1tide	1000	0.45	1	Mg	5
MRCK β	MSA	DAPK1tide	1000	0.67	1	Mg	5
MSK1	MSA	Crosstide	1000	13	10	Mg	5
MSK2 ¹⁾	MSA	Crosstide	1000	40	50	Mg	5
MSSK1 ¹⁾	MSA	DYRKtide-F	1000	56	50	Mg	5
MST1 ¹⁾¹⁰⁾	MSA	IRS1	1000	50	50	Mg	5
MST2 ¹⁾⁶⁾	MSA	IRS1	1000	69	75	Mg	5
MST3 ¹⁾	MSA	Moesin-derived peptide	1000	66	75	Mg	5
MST4 ¹⁾	MSA	Moesin-derived peptide	1000	76	75	Mg	5
NDR1 ¹⁾	MSA	SGKtide	1000	12	10	Mg	5
NDR2 ¹⁾	MSA	SGKtide	1000	7.6	10	Mg	5
NEK1 ¹⁾	MSA	CDK7 peptide	1000	64	75	Mg	5
NEK2	MSA	CDK7 peptide	1000	65	75	Mg	5
NEK4	MSA	GS peptide	1000	51	50	Mg	5
NEK6 ¹⁾	MSA	CDK7 peptide	1000	69	75	Mg	5
NEK7 ¹⁾	MSA	CDK7 peptide	1000	40	50	Mg	5
NEK9 ¹⁾	MSA	CDK7 peptide	1000	190	200	Mg	5
NuaK1	MSA	CHKtide	1000	59	50	Mg	5
NuaK2	MSA	CHKtide	1000	26	25	Mg	5
p38 α	MSA	Modified Erktide	1000	150	150	Mg	5
p38 β	MSA	Modified Erktide	1000	63	75	Mg	5
p38 γ	MSA	Modified Erktide	1000	13	10	Mg	5
p38 δ	MSA	Modified Erktide	1000	5.8	5	Mg	5
p70S6K	MSA	S6k2 peptide	1000	14	10	Mg	5

p70S6K β	MSA	S6k2 peptide	1000	3.3	5	Mg	5
PAK1	MSA	LIMKtide	1000	300	300	Mg	5
PAK2	MSA	DAPK1tide	1000	81	100	Mg	5
PAK4 ¹⁾	MSA	SGKtide	1000	2.5	5	Mg	5
PAK5	MSA	DAPK1tide	1000	1.9	1	Mg	5
PAK6 ¹⁾	MSA	SGKtide	1000	3.7	5	Mg	5
PASK ¹⁾	MSA	GS peptide	1000	9.7	10	Mg	5
PBK ¹⁾	MSA	Histone H3 peptide	1000	33	50	Mg	5
PDHK2 ¹⁾	MSA	PDHKtide	1000	28	25	Mg+K	5+3
PDHK4 ¹⁾	MSA	PDHKtide	1000	19	25	Mg+K	5+25
PDK1 ¹⁾⁷⁾	MSA	T308tide	1000	9.6	10	Mg	5
PEK	IMAP	SRPKtide	100	13	10	Mg	5
PGK ¹⁾³⁾	MSA	Kemptide	1000	8.2	10	Mg	5
PHKG1 ¹⁾	MSA	GS peptide	1000	71	75	Mg	5
PHKG2	MSA	GS peptide	1000	8.1	10	Mg	5
PIM1	MSA	S6k2 peptide	1000	640	500	Mg	5
PIM2 ¹⁾	MSA	S6k2 peptide	1000	4	5	Mg	5
PIM3	MSA	S6k2 peptide	1000	130	150	Mg	5
PKAC α	MSA	Kemptide	1000	2.6	5	Mg	5
PKAC β	MSA	Kemptide	1000	4.7	5	Mg	5
PKAC γ ¹⁾	MSA	Kemptide	1000	4.5	5	Mg	5
PKC α ⁴⁾	MSA	PKC peptide	1000	36	50	Mg+Ca	5+0.05
PKC β 1 ⁴⁾	MSA	PKC peptide	1000	79	75	Mg+Ca	5+0.05
PKC β 2 ⁴⁾	MSA	PKC peptide	1000	41	50	Mg+Ca	5+0.05
PKC γ ⁴⁾	MSA	PKC peptide	1000	74	75	Mg+Ca	5+0.05
PKC δ ⁴⁾	MSA	PKC peptide	1000	26	25	Mg	5
PKC ϵ ⁴⁾	MSA	PKC peptide	1000	16	25	Mg	5

PKC ζ	MSA	PKC peptide	1000	11	10	Mg	5
PKC η ⁴⁾	MSA	PKC peptide	1000	36	50	Mg	5
PKC θ ⁴⁾	MSA	PKC peptide	1000	25	25	Mg	5
PKC ι	MSA	PKC peptide	1000	24	25	Mg	5
PKD1	MSA	GS peptide	1000	25	25	Mg	5
PKD2	MSA	GS peptide	1000	26	25	Mg	5
PKD3	MSA	GS peptide	1000	34	50	Mg	5
PKN1	IMAP	S6K peptide	100	19	25	Mg	1
PKR	IMAP	SRPKtide	100	13	10	Mg	5
PLK1 ¹⁾	MSA	CDC25ctide	1000	5.6	5	Mg	5
PLK2	IMAP	CHK2 peptide	50	30	30	Mg	10
PLK3	MSA	CDC25ctide	1000	6.8	5	Mg	5
PRKX ¹⁾	MSA	Kemptide	1000	20	25	Mg	5
QIK	MSA	AMARA peptide	1000	42	50	Mg	5
RAF1_Cascade	MSA	MAP2K1	1	-	1000	Mg	5
		Erk2	2.5				
		Modified Erktide	1000				
ROCK1	MSA	LIMKtide	1000	3.1	5	Mg	5
ROCK2	MSA	LIMKtide	1000	7.4	5	Mg	5
RSK1	MSA	S6K peptide (N-FL)	1000	21	25	Mg	5
RSK2	MSA	S6K peptide (N-FL)	1000	14	10	Mg	5
RSK3	MSA	S6K peptide (N-FL)	1000	9.9	10	Mg	5
RSK4	MSA	S6K peptide (N-FL)	1000	20	25	Mg	5

SGK	MSA	SGKtide	1000	52	50	Mg	5
SGK2	MSA	SGKtide	1000	58	50	Mg	5
SGK3	MSA	SGKtide	1000	17	25	Mg	5
SIK ¹⁾	MSA	AMARA peptide	1000	47	50	Mg	5
skMLCK ²⁾	MSA	MLCtide	1000	820	1000	Mg	5
SLK ¹⁾	MSA	Moesin-derived peptide	1000	36	50	Mg	5
SRPK1	IMAP	SRPKtide	100	200	100	Mg	10
SRPK2 ¹⁾	MSA	DYRKtide-F	1000	14	10	Mg	5
TAK1-TAB1_Cascade ¹⁾	MSA	MAP2K4 / MAP2K7	0.5 / 0.5	-	1000	Mg	5
		JNK2	50				
		Modified Erktide	1000				
TAOK2 ¹⁾⁶⁾	MSA	TAOKtide	1000	39	50	Mg	5
TBK1	MSA	CKtide	1000	21	25	Mg	5
TNIK	MSA	Moesin-derived peptide	1000	16	25	Mg	5
TSSK1	MSA	GS peptide	1000	11	10	Mg	5
TSSK2 ¹⁾	MSA	GS peptide	1000	8.8	10	Mg	5
TSSK3 ¹⁾	MSA	GS peptide	1000	45	50	Mg	5
WNK1 ¹⁾	MSA	SPAKtide	1000	140	150	Mg+Mn	5+3
WNK2 ¹⁾	MSA	SPAKtide	1000	48	50	Mg+Mn	5+3
WNK3 ¹⁾	MSA	SPAKtide	1000	48	50	Mg+Mn	5+3
PIK3CA/PIK3R1 ¹⁾⁸⁾	MSA	Phosphatidyl- inositol	1000	58	50	Mg	5
SPHK1	MSA	Sphingosine	1000	20	25	Mg	5
SPHK2	MSA	Sphingosine	1000	620	600	Mg	5

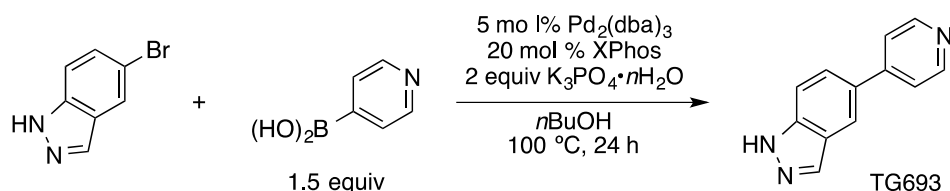
- 1) Reaction time is 5 hours.
- 2) CaCl_2 , Calmodulin are added at the final concentration of 1 mM and 10 $\mu\text{g/ml}$, respectively.
- 3) cGMP is added at the final concentration of 5 μM .
- 4) Phosphatidylserine and Diacyl Glycerol are added at the final concentration of 50 $\mu\text{g/mL}$ and 5 $\mu\text{g/mL}$, respectively.
- 5) Sodium orthovanadate is added at the final concentration of 25 μM .
- 6) Cantharidin is added at the final concentration of 10 μM .
- 7) PIFtide and Cantharidin are added at the final concentration of 2 μM and 20 μM , respectively.
- 8) Assay buffer is 20 mM HEPES(pH 7.5), 2mM DTT. □ Sodium cholate, NaCl and cantharidine are added at the final concentration of 25 μM , 75 mM and 20 μM , respectively.
- 9) TPX2 peptide is added at the final concentration of 200 nM.
- 10) Cantharidin is added at the final concentration of 20 μM .

Supplementary Methods

Chemical Synthesis

General notes: Analytical thin-layer chromatography (TLC) was performed on precoated (0.25 mm) silica-gel plates (Merck Chemicals, Silica Gel 60 F₂₅₄, Cat. No. 1.05715). Preparative thin-layer chromatography (PTLC) was performed on silica-gel (Wako Pure Chemical Industries Ltd., Wakogel B5-F, Cat. No. 230-0043). Melting point (Mp) was measured on an OptiMelt MPA100 automated melting point apparatus (Stanford Research Systems), and is uncorrected. IR spectrum was measured by diffuse reflectance method on a Shimadzu IRPrestige-21 spectrometer attached with DRS-8000A with the absorption band given in cm⁻¹. ¹H and ¹³C NMR spectra were obtained with a Bruker AVANCE 500 spectrometer at 500 and 126 MHz, respectively. CDCl₃ containing 0.03% tetramethylsilane (99.8%D, Kanto Chemical Co. Inc., Cat. No. 07663-23) was used as a solvent for obtaining NMR spectra. Chemical shifts (δ) are given in parts per million (ppm) downfield from (CH₃)₄Si (δ 0.00) as an internal reference with coupling constants (*J*) in hertz (Hz). The abbreviations s and d signify singlet and doublet, respectively. High-resolution mass spectrum (HRMS) was measured on a Bruker micrOTOF mass spectrometer under positive electrospray ionization (ESI⁺) conditions.

5-(4-Pyridinyl)-1*H*-indazole (**TG693**)



Under argon atmosphere, a suspension of 5-bromoindazole (118 mg, 0.601 mmol), 4-pyridylboronic acid (110 mg, 0.898 mmol), Pd₂(dba)₃ (27.5 mg, 30.0 μmol), XPhos (57.6 mg, 0.118 mmol), and K₃PO₄·*n*H₂O (255 mg, <1.20 mmol) in *n*-BuOH (2.4 mL) was stirred for 24 h at 100 °C (oil bath temperature). After cooling to room temperature, the mixture was passed through a short pad of Celite and concentrated under reduced pressure. The obtained orange oil was purified by preparative TLC (CHCl₃/MeOH = 10/1) to give **TG693** (24.4 mg, 0.125 mmol, 20.8%) as a yellow solid.

TLC *R*_f = 0.26 (CH₂Cl₂/MeOH = 20/1); Mp 190 °C (decomp.); IR (cm⁻¹) 792, 798, 802, 1030, 1349, 1420, 1490, 1603, 3361; ¹H NMR (CDCl₃, 500 MHz) δ 7.57 (AA'BB', 2H), 7.62 (d, *J* = 8.5 Hz, 1H), 7.70 (dd, *J* = 1.3, 8.5 Hz, 1H), 8.06 (d, *J* = 1.3 Hz, 1H), 8.18 (s, 1H), 8.68 (AA'BB', 2H) (The signal for *NH* of indazole was not observed); ¹³C NMR (CDCl₃, 126 MHz) δ 110.5, 119.7, 121.4, 121.8, 123.9, 126.3, 131.5, 135.6, 140.2, 150.1; HRMS (ESI⁺) *m/z* 196.0867 ([*M*+*H*]⁺, C₁₂H₁₀N₃ requires 196.0869).

Single dose oral toxicity studies in rats

Male and female 4-week-old Crl: CD (SD) rats were purchased from Charles River Laboratories Inc. After starvation for 6 h, animals were orally administered with TG693 (100 mg kg⁻¹) or the vehicle (0.5% methylcellulose) alone. Gross appearances of animals were observed immediately and after 6 h of the administration and thereafter once a day for 7 days. Body weights were measured at 0, 1, 3, 7 days after oral administration.